Oblique convergence, arc-parallel extension, and the role of strike-slip faulting in the High Himalaya

Richard H. Styron[1,*], Michael H. Taylor[1], and Michael A. Murphy[2]
[1]*Department of Geology, University of Kansas, 1475 Jayhawk Boulevard, Lawrence, Kansas 66045, USA*
[2]*Department of Earth and Atmospheric Sciences, University of Houston, Houston, Texas 77204-5007, USA*

ABSTRACT

Arc-parallel extension is an important component of the active deformation of the Himalaya. This extension is accommodated via arc-perpendicular normal faults linked to arc-parallel strike-slip faults. Analysis of ~130 global positioning system geodetic velocities indicates >3 cm yr^{-1} of arc-parallel extension of the Himalaya. Several models have sought to explain Himalayan arc-parallel extension and strike-slip faulting, including lateral extrusion of Tibet, oroclinal bending of the Himalaya, radial spreading of Tibet and the Himalaya, and variably oblique convergence between India and the Himalaya. Predictions of each model are tested against structural and geodetic observations. These tests indicate that the oblique convergence model best describes Himalayan extensional and strike-slip deformation.

INTRODUCTION

Throughout much of the Phanerozoic, the southern margin of Eurasia has been tectonically active; the collision and subsequent accretion of continental lithospheric fragments against Eurasia since the middle Paleozoic have produced the highly deformed crust that now makes up the orogens of Central Asia (Yin and Harrison, 2000). This process is ongoing; India's Late Cretaceous–early Paleogene collision and continued convergence with Eurasia have produced an active deformation zone extending for >2000 km (Taylor and Yin, 2009). This deformation has uplifted the Himalaya range and portions of the Tibetan Plateau, producing the highest topography on Earth, where most of the Indo-Eurasian relative motion is accommodated (Gan et al., 2007). This convergence is the primary cause for central Asian deformation, though many models have been proposed to explain the observations of the geometry and active tectonics of the Indo-Asian collision zone or subsets of it, especially in Tibet and the Himalaya. These include, but are not limited to, models of rapid uplift of the Tibetan Plateau due to detachment and sinking of the lithospheric mantle (e.g., Molnar et al., 1993); northeast stepwise uplift of Tibet (Tapponnier et al., 2001); gravitationally driven collapse of the plateau (e.g., Dewey, 1988; Jade et al., 2004), possibly accommodated by lower crustal flow from under the plateau to the east (e.g., Royden et al., 1997); viscous (continuous) deformation of Tibetan lithosphere (e.g., England and Houseman, 1988); and deformation of Tibet and the Himalaya via motion of a number of relatively small internally rigid blocks (e.g., Chen et al., 2004a; Meade, 2007; Thatcher, 2007).

Though the Himalayan-Tibetan orogen is often considered the type model of a continental collisional orogen, active shortening structures are limited to the margins of the Tibetan Plateau, essentially the Himalayan front and where the plateau borders the Tarim, Qaidam, and Sichuan Basins (Métivier et al., 1998; Taylor and Yin, 2009). Within Tibet, active deformation is widespread and consists of east-directed extension, accommodated by generally north-striking rifts and coeval north-south shortening via conjugate northeast- and northwest-striking strike-slip faults (Armijo et al., 1986, 1989; Taylor et al., 2003; Taylor and Yin, 2009) (Fig. 1). Active normal and strike-slip faulting is present within the Himalayan arc as well; these show slip directions to be generally arc parallel, resulting in both arc-parallel extension and translation (Nakata, 1989; Murphy et al., 2002, 2009; Murphy and Copeland, 2005; Thiede et al., 2006; Jessup et al., 2008; Li and Yin, 2008). Various mechanisms have been proposed to explain deformation in the Himalaya and south Tibet, including lateral extrusion of a rigid Tibet along the Karakoram fault (KF) and Indus-Yarlung suture zone (IYS) (Tapponnier et al., 1982; Lacassin et al., 2004); oroclinal bending (Li and Yin, 2008); outward radial expansion of the Tibetan Plateau (Molnar and Lyon-Caen, 1989; Copley and McKenzie, 2007; Murphy et al., 2009); and variably oblique Indo-Himalayan convergence (McCaffrey and Nábelek, 1998; Seeber and Pêcher, 1998). These models are described in more detail in the following, and specific, testable predictions of each are presented.

Here we combine and analyze several recently published global positioning system (GPS) geodetic data sets in the Himalaya and immediate surroundings to evaluate the arc-parallel and arc-normal components of the velocity field in the Himalaya. We then use these results and structural observations from the geologic literature on the Himalaya and south Tibet to evaluate the more prominent models for modern Himalayan deformation.

ACTIVE STRUCTURES OF THE HIMALAYA AND SOUTH TIBET

Both the Himalaya and south Tibet show widespread active extensional and strike-slip faulting, though there are differences in deformational style. Active deformation in central Tibet consists of approximately east-west extension accommodated within the Lhasa and Qiangtang blocks via north-south–striking rifts (Armijo et al., 1986, 1989; Yin et al., 1999a) (Figs. 1 and 2). Near the Bangong-Nujiang suture zone, the rifts link with conjugate northwest-striking dextral faults and northeast-striking sinistral faults that merge with the Bangong-Nujiang suture zone (Armijo et al., 1989), which accommodates north-south shortening and potentially more rapid east-west extension and eastward advection of central Tibetan lithosphere (Taylor et al., 2003; Taylor and Peltzer, 2006). In the central Lhasa block, several of the major rifts cut southward through the IYS into the Himalayan arc (Yin, 2000). From east to west (Fig. 2), these include the Yadong-Gulu rift (Cogan et al., 1998), the Pum

*Corresponding author: styron@ku.edu.

Geosphere; April 2011; v. 7; no. 2; p. 582–596; doi: 10.1130/GES00606.1; 10 figures; 1 table; 1 supplemental table.

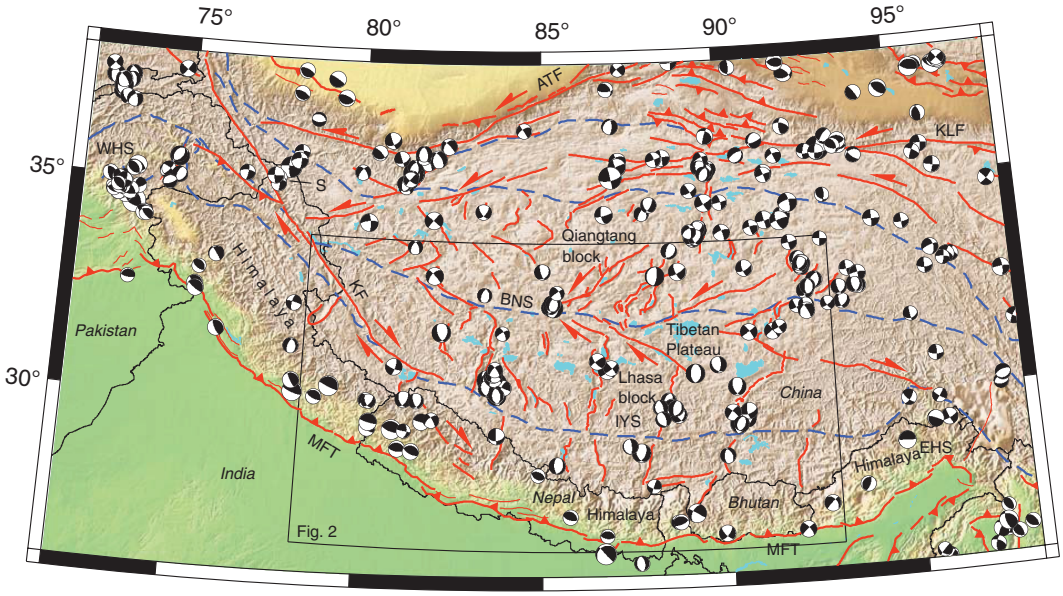

Figure 1. Active structures (orange lines) and suture zones (dashed blue lines) of the Himalayan-Tibetan orogen (after Styron et al., 2010). Focal mechanisms are from the Global Centroid Moment Tensor catalog (www.globalcmt.org), 1976–2008. Topography is from the Shuttle Radar Topography Mission. MFT—Main Frontal thrust; WHS—western Himalayan syntaxis; EHS—eastern Himalayan syntaxis; IYS—Indus-Yarlung suture; KF—Karakoram fault; BNS—Bangong-Nujiang suture; ATF—Altyn Tagh fault; S—global positioning system site STAKSHA; KLF—Kunlun fault.

Qu–Xainza rift (Hager et al., 2006) (which may link to the south with the Nyönno Ri detachment bounding the Ama Drime Massif; Jessup et al., 2008; Kali et al., 2010), the Tangra Yum Co–Tingri rift (Dewane et al., 2006; Taylor and Yin, 2009), the Kung Co rift (Mahéo et al., 2007; Lee et al., 2011), and the Lopukangri rift (Murphy et al., 2010). Active rifting in the Lhasa block is not documented in western Tibet north of the KF, nor does this area display seismicity indicative of extension (Fig. 1).

Active deformation in the Himalaya involves both extension and strike-slip faulting (Figs. 1 and 2), though the orientation of the strain field is much more variable than in Tibet (Gan et al., 2007). The dominant active structures within the Himalaya (north of the Main Frontal thrust) are those accommodating arc-parallel extension (although studies have suggested recent activity of the Main Central thrust; e.g., Hodges et al., 2004). Major active structures in the northwest Himalaya include the Leo Pargil core complex in northwest India, which is bound in the north by the KF and has accommodated some tens of kilometers of extension (Thiede et al., 2006), and the Gurla Mandhata core complex, which has been interpreted to be a releasing bend in the right-lateral Karakoram-Humla fault system (Murphy and Copeland, 2005), and has accommodated 24–60 km extension, depending on the geometry of the core complex's major detachment at depth. The central Himalaya contains rifts cutting the range, such as the southern reaches of the south Tibetan rifts mentioned here, and the Thakkhola graben (Hurtado et al., 2001). With the exception of the Ama Drime Massif (Jessup et al., 2008), with a provisional extension estimate of 18–36 km on the western range-bounding Ama Drime detachment and 15–30 km on the eastern Nyönno Ri detachment, these rifts do not generally show the high magnitudes of extension of the western systems; estimates are often ~10 km (Mahéo et al., 2007; Wu et al., 1998).

Active strike-slip faulting has been described throughout much of the Himalaya. In northwestern India, northwest-striking right-slip faults are associated with and often linked to east- and west-dipping normal faults (Steck et al., 1998; Clark, 2005; Epard and Steck, 2008), including the Leo Pargil core complex (Thiede et al., 2006) and arc-parallel dextral shear zones (Vannay and Steck, 1995; Epard and Steck, 2004). Farther to the southeast, dextral arc-parallel strike-slip faulting has been observed in a zone from Gurla Mandhata southeast into the Himalayan foothills in central Nepal. In Murphy and Copeland (2005), a right-slip fault was mapped, named the Humla fault, extending east from the southern margin of Gurla Mandhata (Fig. 2). The Gurla Mandhata–Humla fault system has been interpreted to transfer slip along the KF into the Himalaya (Murphy and Copeland, 2005; Murphy and Burgess, 2006). The Humla fault may then feed slip into an en echelon system of active dextral faults, including the Tibrikot, Dhaulagiri Southwest, and Bari Gad faults (Nakata, 1989; Styron et al., 2009; Murphy et al., 2010).

The KF is the longest and most studied of the arc-parallel dextral faults in the western Himalaya region. The KF forms the boundary between the actively extending northwest Himalaya and the relatively rigid southwest Tibet. Estimates of geologic offsets along the KF vary greatly. Initial estimates based on early mapping and tentative correlations of large-scale features such as batholiths (e.g., ~1000 km; Peltzer and Tapponnier, 1988) are significantly higher than more recent estimates, but even the recent estimates have significant variability. Although some of these are incompatible, as they are based on correlations of one offset feature on one side of the fault with different features on the opposite side of the fault (e.g., Lacassin et al., 2004; cf. Searle, 1991), the lower set of slip estimates, which typically involve correlating narrower and more unique offset features (e.g., Murphy et al., 2000; Robinson, 2009), may be reconciled by the recognition that slip may not be consistent along strike due to internal deformation of the crust to either side of the fault. Robinson (2009) compiled estimates of geologic offsets from locations distributed along much of the KF. These offsets are based on separation of a variety of features, including sedimentary and igneous rock bodies, fault and suture zones, and the course of the Indus River (Murphy and Copeland, 2005; Murphy et al., 2000, 2002; Searle, 1996; Searle et al., 1998; Phillips et al., 2004; Robinson, 2009). These offsets are plotted with respect to distance along strike of the arc in Figure 3. If these offset estimates are accurate, the Himalaya has undergone significant (>100 km) extension where bounded by the KF. Although it has often been suggested that slip along the KF feeds into the IYS, it was found (Murphy et al., 2010) that the northern margin of the IYS is cut and offset 15 km by the Lopukangri rift system. This westernmost disruption of the IYS by north-trending rifts in

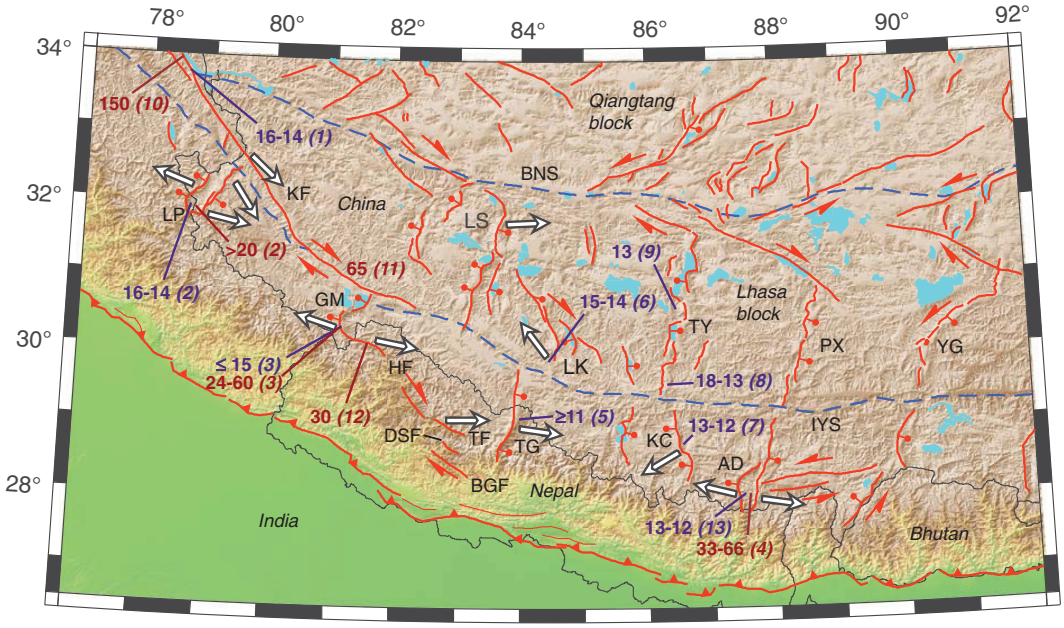

Figure 2. Active structures (orange lines) and sutures (dashed blue lines) (after Styron et al., 2010; Thiede et al., 2006; Jessup et al., 2008). LP—Leo Pargil dome; GM—Gurla Mandhata dome; HF—Humla fault; KF—Karakoram fault; BGF—Bari Gad fault; DSF—Dhaulagiri Southwest fault; TF—Tribrikot fault; TG—Thakkhola graben; KC—Kung Co rift; AD—Ama Drime Massif; IYS—Indus-Yarlung suture; LK—Lopukangri rift; LS—Lunggar Shan rift; TY—Tangra-Yumco rift; PX—Pum Qu-Xainza rift; YG—Yadong-Gulu rift; BNS—Bangong-Nujiang suture. Numbers in purple indicate initiation ages (Ma). Numbers in reddish-brown indicate fault heave (km). Sources are given in italics. 1—Phillips et al. (2004); 2—Thiede et al. (2006); 3—Murphy et al. (2002); 4—Langille et al. (2010); 5—Garzione et al. (2003); 6—Murphy et al. (2010); 7—Lee et al. (2011); 8—Williams et al. (2001); 9—Dewane et al. (2006); 10—Searle (1996); 11—Murphy et al., 2000); 12—Murphy and Copeland (2005); 13—Kali et al. (2010). Arrows indicate mean azimuth of fault heave, relative to the footwall in the case of nonvertical faults. Fault slip data sources: KF—Murphy et al. (2009); LP—Thiede et al. (2006); GM—Murphy et al. (2002); LS—Sundell et al. (2010); LK—Murphy et al. (2010); TF—Styron et al. (2009); TG—Baltz and Murphy (2009); KC—Lee et al. (2011); AD—Jessup et al. (2008), Kali et al. (2010). Topography is from Shuttle Radar Topography Mission.

addition to the central Himalayan examples of rifting of the IYS cited here strongly suggest that the IYS has hosted no significant strike-slip motion since the Middle Miocene, and that KF slip is transferred to the south into the Himalaya along the Gurla Mandhata–Humla fault system.

Significant right-lateral arc-parallel strike-slip faulting in the Himalaya has not been described east of the Bari Gad fault (Fig. 2). Rather, strike-slip faulting becomes left lateral east of central Nepal. Strike-slip motion is taken up both by discrete arc-parallel sinistral structures (Li and Yin, 2008) and transtensional faults such as segments of the Yadong-Gulu rift (Armijo et al., 1986; Kapp and Guynn, 2004) (Figs. 1 and 2). Focal mechanisms suggest steeply dipping, arc-parallel left-lateral faulting in Bhutan (Drukpa et al., 2006). These sinistral faults are somewhat less organized than the dextral faults of the western Himalaya and probably have accommodated significantly smaller amounts of translation (Li and Yin, 2008).

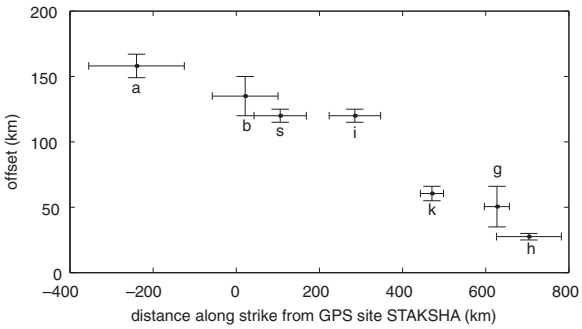

Figure 3. Offset estimates of geologic features along the Karakoram–Humla fault system plotted by their distance along strike of the Himalayan arc from global positioning system site STAKSHA (34.82°N, 77.52°E; Fig. 1), as compiled in Robinson (2009). Errors on the x axis correspond to the along-strike distance spanned by the offset features. Errors on the y axis indicate the error associated with the estimated offset. a—Aghil limestone; b—Baltoro granite; s—Shyok suture; i—Indus River; k—South Kailas thrust; g—Gurla Mandhata detachment; h—Humla fault. See text for sources.

Timing of Initiation of Extension

Figure 2 shows published age estimates that bracket the time initiation of syncollisional extension and strike-slip faulting. Studies of the Ama Drime Massif utilizing $^{40}Ar/^{39}Ar$ dating of micas and (U-Th)/He dating of apatite suggest the inception of arc-parallel extension at 13–12 Ma, immediately following the local cessation of activity on the Main Central thrust and South Tibetan detachment (Jessup et al., 2008; Kali et al., 2010). Thermochronologic analysis of the Kung Co granite in the footwall of the Kung Co fault by Lee et al. (2011) led to an interpretation involving initiation of normal faulting at 13–12 Ma and acceleration of fault-assisted exhumation at 10 Ma. The Thakkhola graben is the most physiographically prominent graben in the Himalaya. Geologic mapping since the 1970s by Bordet et al. (1971) and Colchen et al. (1986) showed that it is bounded on the west by a major east-dipping normal fault referred to as the Dangardzang fault (DF). Little is known about the thermal history of its footwall, but investigations of its basin fill (Tetang and overlying Thakkhola Formations) preserved in its hanging wall show that it is syndeformational. The older Tetang Formation is between 11 and 9.6 Ma (Garzione et al., 2003), implying that slip along the Dangardzang fault was active at this time, and that it initiated some time before 11 Ma. At its southern end, the Dangardzang fault cuts the Dhaulagiri-Annapurna

detachments (the local segments of the South Tibetan detachment). In the Annapurna and Dhaulagiri ranges, structural, metamorphic, and intrusive histories of rocks exposed on either side of the South Tibetan detachment indicate that it was moving between 22 and 16 Ma (Hodges et al., 1996; Godin et al., 2001; Searle and Godin, 2003; Searle, 2010), thereby placing an upper age constraint on the timing of extension within the Thakkhola graben.

West of Thakkhola, the two most prominent, large-scale active extensional fault systems, the Gurla Mandhata–Humla fault system and the Leo Pargil shear zone, were geochronologically and thermochronologically investigated. Th-Pb monazite dating of mylonitic leucogranite dikes within the Gurla Mandhata–Humla system bracket the timing of ductile extension between 15 and 7 Ma (Murphy and Copeland, 2005). The $^{40}Ar/^{39}Ar$ analyses of white mica and biotite from rocks in the footwall of the Leo Pargil shear zone are interpreted to reflect the onset of fault-facilitated exhumation ca. 15 Ma (Thiede et al., 2006). The KF borders both of these extensional systems to the north and is kinematically linked, at least in the case of the Gurla Mandhata–Humla system (Murphy et al., 2002). Near Banggong Co, U-Pb zircon dating of syndeformational granite bodies brackets the time of initiation between 15.68 ± 0.52 and 13.73 ± 0.28 Ma (Phillips et al., 2004). Lacassin et al. (2004) and Valli et al. (2007) estimated much older ages for the timing of initiation along the KF (23–34 Ma). Zhang et al. (2010) showed through geologic mapping that rocks and structures (Great Counter thrust) they associate with the KF are part of an older structural system referred to as the Ayi Shan detachment.

These data together indicate a common Middle Miocene initiation of arc-parallel extension and translation throughout the central and northwestern Himalaya.

Tibrikot Fault

Nakata (1989) recognized the presence of active right-lateral strike-slip faulting in the western Nepalese Himalaya, and documented the Tibrikot, Dhaulagiri Southwest, and Bari Gad faults through remote sensing and field observations (Fig. 2). Preliminary field observations of the arc-parallel Tibrikot fault (Styron et al., 2009) indicate late Quaternary dextral slip on a steeply dipping arc-parallel fault near the base of the Main Central thrust zone. Both bedrock and fluvial geomorphic features are clearly offset in a right-lateral sense, as shown in Corona satellite imagery (Fig. 4). The fault zone is narrow, and shows brittle deformation, in contrast to the ductilely deformed rocks it cuts. Though net slip on the Tibrikot is unknown, the short length of the fault suggests that displacement is lower than on other arc-parallel strike-slip faults in the Himalaya, such as the KF, and likely younger.

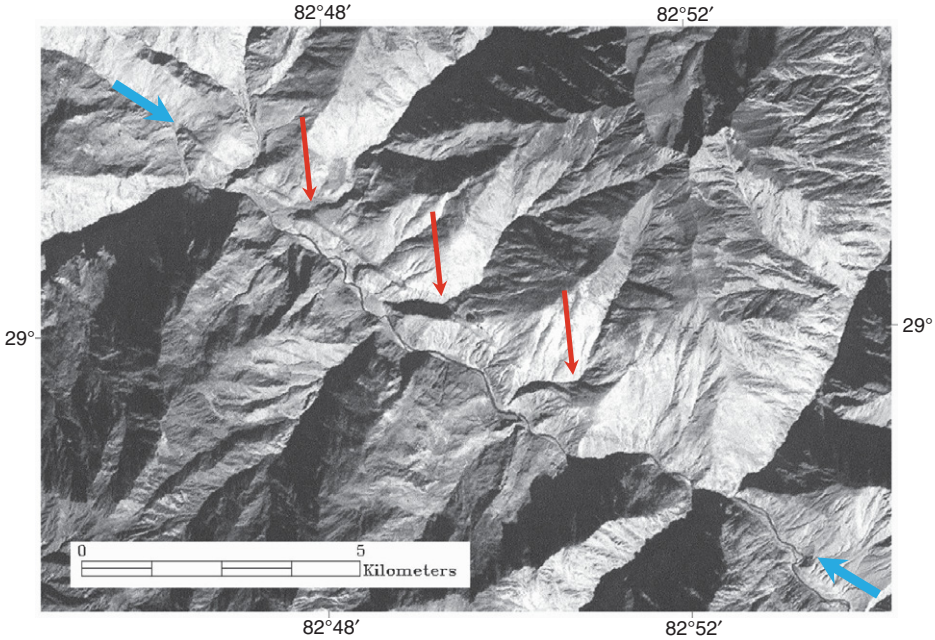

Figure 4. Corona satellite imagery of the Tibrikot fault, Dolpo region, Nepal. Blue arrows indicate the trace of the fault. Red arrows indicate consistent right-lateral offsets of stream drainages crossing the fault. Note the sharpness of the fault trace, which suggests its recent activity.

The Tibrikot fault geometry, kinematics, and location in a zone of right-lateral shear strongly suggest that the fault represents the propagation of KF slip from the IYS region through the High Himalaya via the Gurla Mandhata–Humla system and into the frontal Himalaya. Though displacement is likely relatively small, the Tibrikot appears to be a significant structure as it and adjacent dextral faults appear to represent the propagation of KF slip through the Himalaya instead of along the IYS, which has implications for the validity of models of Himalayan and south Tibetan deformation outlined in the following.

MODELS FOR HIMALAYAN AND SOUTH TIBETAN ACTIVE DEFORMATION

The recent decades of research in the Indo-Asian collision zone have produced several models to explain the multifaceted deformation in the region. Several of the most common models are briefly discussed here, along with specific predictions that may be tested with the observations and analysis presented in this work. It is important to note that these predictions may or may not have been explicitly discussed by any of the researchers who published the models; however, we feel that these predictions come directly out of the models.

Lateral Extrusion

The lateral extrusion model of Indo-Asian tectonics was one of the first models put forth to explain the first-order structural features of the Tibetan Plateau and its surrounding areas visible in early satellite images (e.g., Tapponnier et al., 1982). Essentially, this model describes Tibet as undergoing tectonic escape and translating eastward relative to stable Eurasia and India as India indents into Asia. The lateral extrusion of Tibet is accommodated along the left-lateral Altyn Tagh and Kunlun faults in the north (Fig. 1) and the right-lateral KF and right slip along the IYS in the south (Tapponnier et al., 1982; Lacassin et al., 2004; Schill et al., 2004; Valli et al., 2007, 2008). While this model was not initially proposed to explicitly explain deformation in the Himalaya, it implies high magnitudes of slip and slip rate along the KF continue as dextral shear into the IYS (Fig. 5A).

Oroclinal Bending

The oroclinal bending model describing the curvature of the Himalayan arc involves rotational bending of an initially linear belt. The

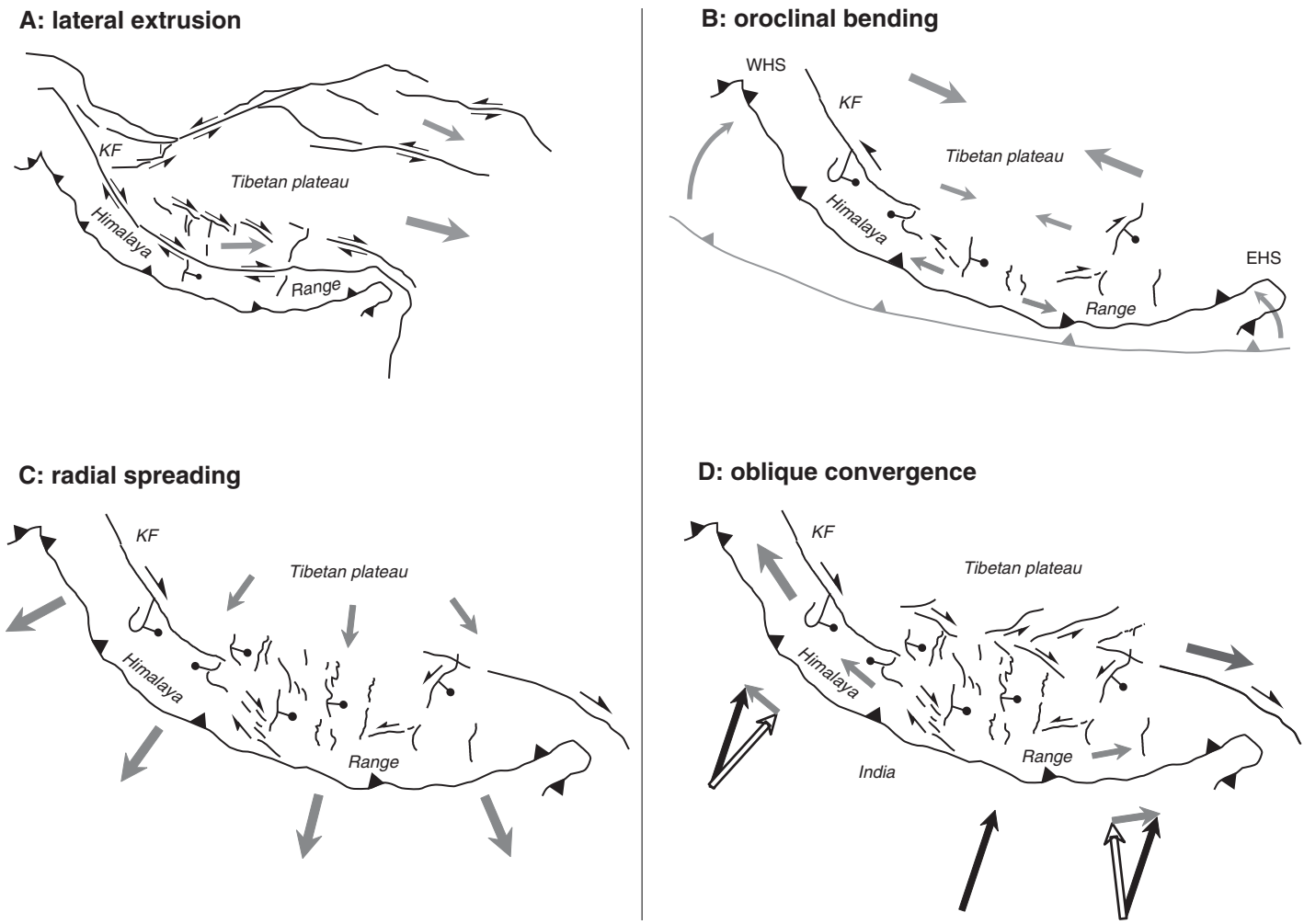

Figure 5. Models for Himalayan and south Tibetan deformation. (A) Lateral extrusion model, where the Tibetan Plateau translates to the east (gray arrows) along right-lateral structures along its southern margin and left-lateral structures along its northern margin. KF—Karakoram fault. (B) Oroclinal bending model, where the Himalayan orogen bends such that the Eastern Himalayan syntaxis (EHS) and the Western Himalayan syntaxis (WHS) move toward each other, resulting in a decrease in the radius of curvature of the Himalayan arc. This causes extension of the outer (India facing) Himalaya and contraction of the interior of the orogen (gray arrows), and strike-slip faulting analogous to flexural slip. (C) Radial spreading model, where Tibet expands radially to the south (gray arrows), causing arc-parallel extension of the Himalaya. (D) Oblique convergence model, where India's motion relative to Eurasia (black arrows) has an arc-normal component (white arrows) and arc-parallel component (gray arrows), causing arc-parallel extension and translation of the Himalaya. The dark gray arrow represents the eastward motion of central Tibetan lithosphere independent of oblique convergence.

primary lines of evidence for this process are clockwise paleomagnetic rotations in the northwest Himalaya (e.g., Klootwijk et al., 1985; Schill et al., 2001, 2002) and right-lateral arc-parallel faulting in the western Himalaya and adjacent Tibet mirrored by left-lateral faulting in the eastern Himalaya and southern Tibet (e.g., Ratschbacher et al., 1994; Li and Yin, 2008). The predictions for this model vary based on the locations of the hinge lines around which the range rotates, and the mechanism by which this folding occurs, i.e., neutral surface folding or flexural slip. Flexural flow may be a viable mechanism for oroclinal bending at depth, but the upper crust is not expected to shear ductilely; therefore, the brittle upper crust would deform by faulting localizing the distributed shear below, replicating the effects of flexural slip. Other models (Schill et al., 2001, 2002; Li and Yin, 2008) have the Himalayan arc bending around its central part such that the Himalayan syntaxes approach each other and the arc becomes more folded in map view. The kinematic predictions that arise for neutral surface folding are (1) there will be east-west contraction across southern Tibet, and potentially (2) arc-parallel extension in the outer (India-facing) Himalaya decreasing to a region of no extension or contraction along the center of the orocline (analogous to extension in the outer part of a fold's hinge and contraction in the inner part). For flexural slip, the prediction is (3) arc-parallel strike-slip faulting along preexisting structural discontinuities such as the IYS or the faults in the Himalaya, such as those in the Main Central thrust or South Tibetan detachment zones, analogous to flexural slip in folded sedimentary layers. Given the geometry of the orogen, the arc-parallel strike-slip faults west of the central Himalaya would be sinistral and the faults east of the hinge zone would be dextral (Fig. 5B).

Radial Spreading

The Tibetan Plateau's extremely hot, thick crust may be capable of lateral flow at geodetically observable velocities (Bird, 1991; Beaumont et al., 2004). Consequently, Tibet has been proposed to be flowing toward its margins to reduce the gravitational potential energy excess caused by the ~5 km elevation difference between the plateau and its surroundings (e.g., England and Houseman, 1988; Copley and McKenzie, 2007; Copley, 2008; Cook and Royden, 2008). In the radial spreading model of Himalayan deformation, this applies to the Himalayan margin as well as the eastern margin of the plateau. As Tibet spreads out southward over India, it causes radial as well as circumferential expansion (Jade et al., 2004; Murphy and Copeland, 2005; Copley and McKenzie, 2007; Copley, 2008). The following predictions may be made from this model. (1) As Tibet expands toward India, the circumference of the Himalayan arc will expand, causing arc-parallel extension. (2) South-directed radial spreading of the Tibetan Plateau will result in approximately north-south extension, so the Himalaya will move south with respect to both stable Eurasia and to the central Tibetan Plateau. Some researchers have modified this model to allow for a presumably more viscous northwest Himalaya to act as a gate or barrier, allowing the less viscous interior of Tibet to pour out past the Himalaya along the KF, so that (3) right-lateral, arc-parallel strike-slip faulting between the northwest Himalaya and Tibet occurs (Murphy et al., 2002, 2009; Murphy and Copeland, 2005), though this prediction is not necessarily a part of the radial spreading model, especially as envisaged with a rheologically homogeneous Tibet and Himalaya (e.g., Copley and McKenzie, 2007) (Fig. 5C).

Oblique Convergence

The model for Himalayan deformation caused by the variation in convergence obliquity is based on two observations: (1) there is a smooth variation in the strike of the Himalayan arc from the eastern to the western syntaxes, between which the arc may be approximated by a small circle, as judged by several criteria (Bendick and Bilham, 2001); and (2) India-Asia convergence vectors (relative to Asia) are generally parallel, and are normal to the strike of the Himalaya only in the Everest region of Nepal. Therefore, there is an increasing arc-parallel component to the convergence vectors away from the central Himalaya, which causes arc-parallel extension. Arc-parallel extension is most rapid where the along-strike rate of change of the arc-parallel velocities is highest. In the northwestern (and potentially eastern) regions of the Himalaya, the arc is translating along the Himalaya-Tibet boundary, approximated by the KF zone (McCaffrey and Nábelek, 1998; Seeber and Pêcher, 1998). This requires the net slip and slip rate along the KF to increase to the northwest, analogous to a translating and extending forearc sliver such as that observed in Sumatra (McCaffrey, 1992). This model is very commonly applied at subduction zones worldwide (e.g., McCaffrey, 1992; Avé Lallemant and Oldow, 2000), which are almost always convex toward the underthrusting plate, as observed in the Himalaya. Seeber and Pêcher (1998) referred to the pattern of earthquake slip vectors along the Himalaya as reflecting "radial thrusting." Despite the similarity of the terminology, this is distinct from the radial spreading model discussed here; radial thrusting simply refers to the radial orientation of thrust slip vectors, which are normal to the strike of the arc. It does not imply that the radius of the arc grows during thrusting, only that the divergence in slip vectors causes circumferential or arc-parallel extension along the range. This is complemented by contraction at the syntaxes, and accommodated by right-lateral slip along the KF, which strikes roughly normal to the thrust events along the northwestern range front, consistent with slip partitioning. Unlike the oroclinal bending and radial spreading models, the oblique convergence model does not propose to explain the curvature of the Himalayan arc; this model only shows the consequences of the regular variation of Indo-Himalayan convergence obliquity along the arc. The oblique convergence model makes the following testable predictions: (1) the gradient observed in arc-parallel geodetic velocities away from the region of pure normal Indo-Himalayan convergence in eastern Nepal is correlated with the degree of convergence obliquity; (2) there is significant arc-parallel extension in the Himalaya; and (3) arc-parallel extension in the northwest Himalaya is accommodated by arc-parallel strike-slip faults and arc-perpendicular normal faults (Fig. 5D).

GEODETIC ANALYSIS

The most spatially and temporally comprehensive geodetic data set for the Himalayan-Tibetan system yet published is that of Gan et al. (2007), a compilation of the data sets of Zhang et al. (2004), Paul et al. (2001), Wang et al. (2001), and Banerjee and Bürgmann (2002). This set of ~1300 GPS vectors in and around China is given in both a Eurasia-fixed reference frame in the International Terrestrial Reference Frame 2000 (ITRF2000), and a Tibet-fixed reference frame. GPS vectors from the Eurasia-fixed data set in and around the Himalaya were selected. Several other data sets were compiled to increase data coverage and density. Jade et al. (2004) presented a network of GPS vectors in Ladakh and far western Xizang, relative to ITRF97. These data were transformed into ITRF2000 using the National Geodetic Survey's Horizontal Time Dependent Positioning tool (http://www.ngs.noaa.gov/TOOLS/Htdp/Htdp.shtml). Additional GPS data from Bettinelli et al. (2006) and Banerjee et al. (2008) were included. These three data sets were then transformed into a Eurasia-fixed reference frame by using the ITRF2000-Eurasia Euler pole at 57.965 ± 1.211°N, –99.374 ± 2.71°E of Altamimi et al. (2002).

Convergence between India and Eurasia was described by Jade et al. (2007) by a rotation of 0.341° ± 0.005° m.y.$^{-1}$ around a pole at 26.5 ± 3.4°N, 13.9 ± 7.8°E. These rotation parameters were used to generate convergence vectors between India and Eurasia in a Eurasia-fixed reference frame at every GPS site; these are referred to as the plate motion vectors.

The observed geodetic and predicted plate motion vectors are shown in Figure 6. A comparison of the geodetic and plate motion vectors illustrates the degree and spatial extent to which the overriding plate is moving with underthrusting India. Along the Himalayan front, the vectors are very similar. Farther inboard of the thrust front, the velocity of the geodetic vectors lessens as strain is accumulated across the arc, though the vectors generally remain parallel to each other and to the Indo-Asian plate motion vectors. Previous studies can explain the observed velocities with elastic strain accumulation along the Main Himalayan thrust with a locking depth of ~20 km (e.g., Jouanne et al., 1999; Larson et al., 1999; Lavé and Avouac, 2000; Chen et al., 2004a, 2004b). It is also clear that the geodetic vectors are oriented purely normal to the Himalayan arc only in eastern Nepal; convergence is progressively more oblique along strike in either direction. The largest divergence between the geodetic and plate motion vectors is near the eastern Himalayan syntaxis, where there appears to be significant clockwise vertical-axis rotation, also consistent with previous studies (Shen et al., 2005; Allmendinger et al., 2007). Some of this divergence may also be explained by the absorption of a fraction of the total Indo-Asian convergence within the Shillong Plateau (e.g., Banerjee et al., 2008; Clark and Bilham, 2008; cf. Jade et al., 2007).

The consequence of the observed variation in convergence obliquity is that the arc-normal and arc-parallel components to Indo-Himalayan relative motion vary systematically along the

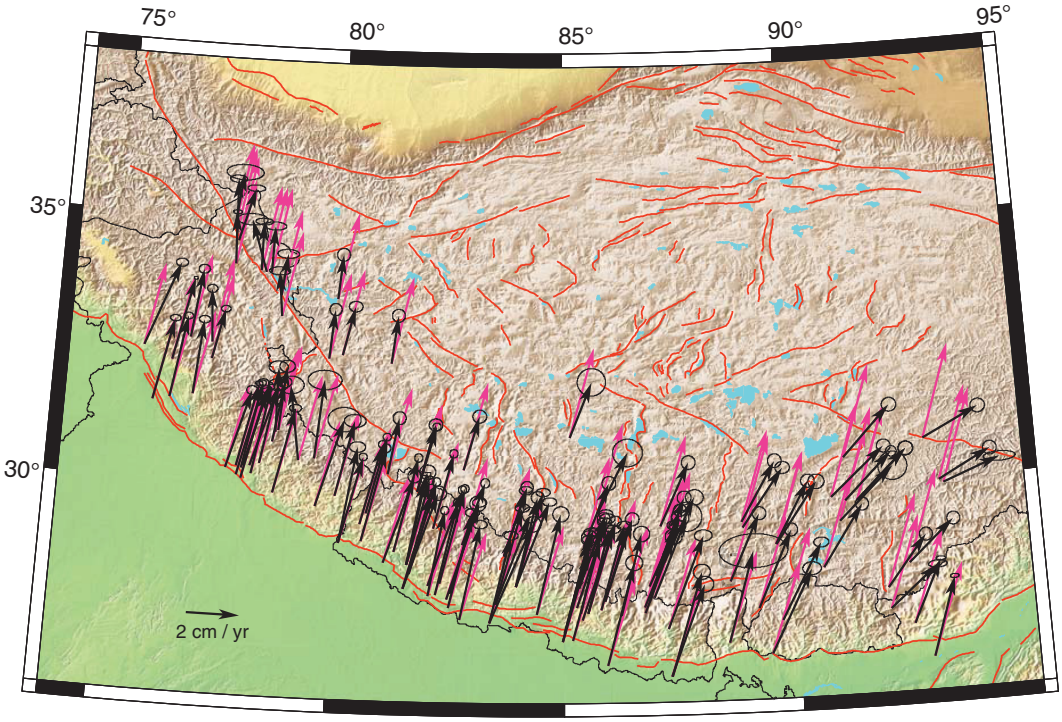

Figure 6. Observed global positioning system (GPS) velocities (black) relative to stable Eurasia in the ITRF2000 reference frame and predicted India-Eurasia plate motion vectors (pink) relative to stable Eurasia in ITRF2000 at each GPS station using the India-Eurasia pole of rotation from Jade et al. (2007). All velocities are plotted using the same scale. Where the GPS and plate motion vectors are similar, the upper crust moves with the Indian plate (locked Main Himalayan thrust). Where the GPS vectors are smaller (slower) than the plate motion vectors but still parallel (such as the interior of Tibet), strain accumulation of the upper plate between the Main Frontal thrust and the GPS site takes place at a rate equal to the difference of the vector magnitudes at that site. The significant divergence in the azimuths of the GPS and plate motion vectors in south Tibet indicates vertical-axis rotation around the Eastern Himalayan syntaxis.

arc. Though the amount of Indo-Himalayan convergence obliquity varies significantly along strike, the seismic events along the Himalayan front have slip vectors dominantly oriented perpendicular to the strike of the arc (Seeber and Pêcher, 1998; Bendick et al., 2007; Fig. 1), not oblique and in the direction of plate convergence and elastic strain accumulation. The few focal mechanisms along the KF or the arc-parallel strike-slip faults in Nepal are also strike slip, not oblique slip. From a geologic perspective, the presence of a large thrust or system of thrust faults (the Main Frontal and Main Boundary thrusts) in the frontal Himalaya and arc-parallel strike-slip faults (the KF, Humla, Tibrikot, and Bari Gad faults) farther inboard, as well as normal faults striking perpendicular to the arc, all suggest that strain in the Himalayan arc is partitioned into fairly pure arc-normal shortening and arc-parallel extension and translation along discrete fault systems. Therefore, in a region where convergence between the Indian plate and the Himalaya is oblique, a thrust event along the Main Frontal thrust will only relieve the arc-normal component of the elastic strain field; the arc-parallel component will only be relieved by an event on a strike-slip fault such as the KF.

In order to assess this quantitatively, each geodetic vector is decomposed into its arc-parallel and arc-normal components, using the definition of the arc as a small circle with a pole at 91.6°E, 42.4°N of Bendick and Bilham (2001) for the western and central segments of the arc, a pole at 89.5°E, 37°N for sites between 88°E to 91.5°E, and a pole at 90.7°E, 35°N for sites west of 91.5°E. The latter two poles are necessary because the radius of curvature for the Himalayan arc decreases east of Sikkim and a small circle about the first pole does not fit the observed arc geometry, and were fit visually. The arc-normal vector is the component of the geodetic velocity in the direction of the pole, and the arc-parallel vector is the velocity component tangential to the small circle at that point. The GPS velocities are available in Supplemental Table 1[1]. The arc-parallel vectors are shown in Figure 7A. Figure 7B shows the arc-parallel velocities within the Himalayan arc (between the KF-IYS and the Main Frontal thrust) plotted with respect to their distance along strike (where the position of each is projected onto a small circle approximating the Himalayan arc of radius 1696 km around the pole of Bendick and Bilham (2001). Although the full two-dimensional velocity error ellipses are shown in the maps, the one-dimensional error bars shown in the plots are calculated as the diameters of the 1 σ error ellipses in the direction of the velocity vectors.

The arc-parallel velocities suggest that the Himalayan arc is stretching at ~3 cm/yr between the India-Pakistan border and the western border of Bhutan. This is ~1500 km along strike, leading to an extension rate of 20 nstrain yr^{-1}. The extension rate is not completely uniform along strike; the sites in the northwesternmost 400 km of the arc have similar arc-parallel velocities, ~20 mm yr^{-1}. However, from near ~78°E to ~89°E (400 km to 1400 km along-strike distance from GPS site STAKSHA), the velocity gradient is fairly uniform, representing ~35 nstrain yr^{-1} of extension (Fig. 7B). The ~10 mm yr^{-1} extension rates from the Humla fault region northwest through the end of the study area broadly agree with >100 km arc-parallel extension of this region (based on the KF displacement gradient) given a Middle Miocene age for the onset of extension.

It is interesting to study how these velocities change across the arc rather than along it. Therefore the arc is divided into seven regions along strike (Fig. 7A), and the arc-normal and arc-parallel components of the GPS site velocities in each region are binned and plotted with respect to their distance from the pole of Bendick and Bilham (2001) (Fig. 8). For each region, the mean arc-parallel and arc-normal velocities for several sites in the Himalayan

[1]Supplemental Table 1. Excel file of GPS velocities. If you are viewing the PDF of this paper or reading it offline, please visit http://dx.doi.org/10.1130/GES00606.S1 or the full-text article on www.gsapubs.org to view Supplemental Table 1.

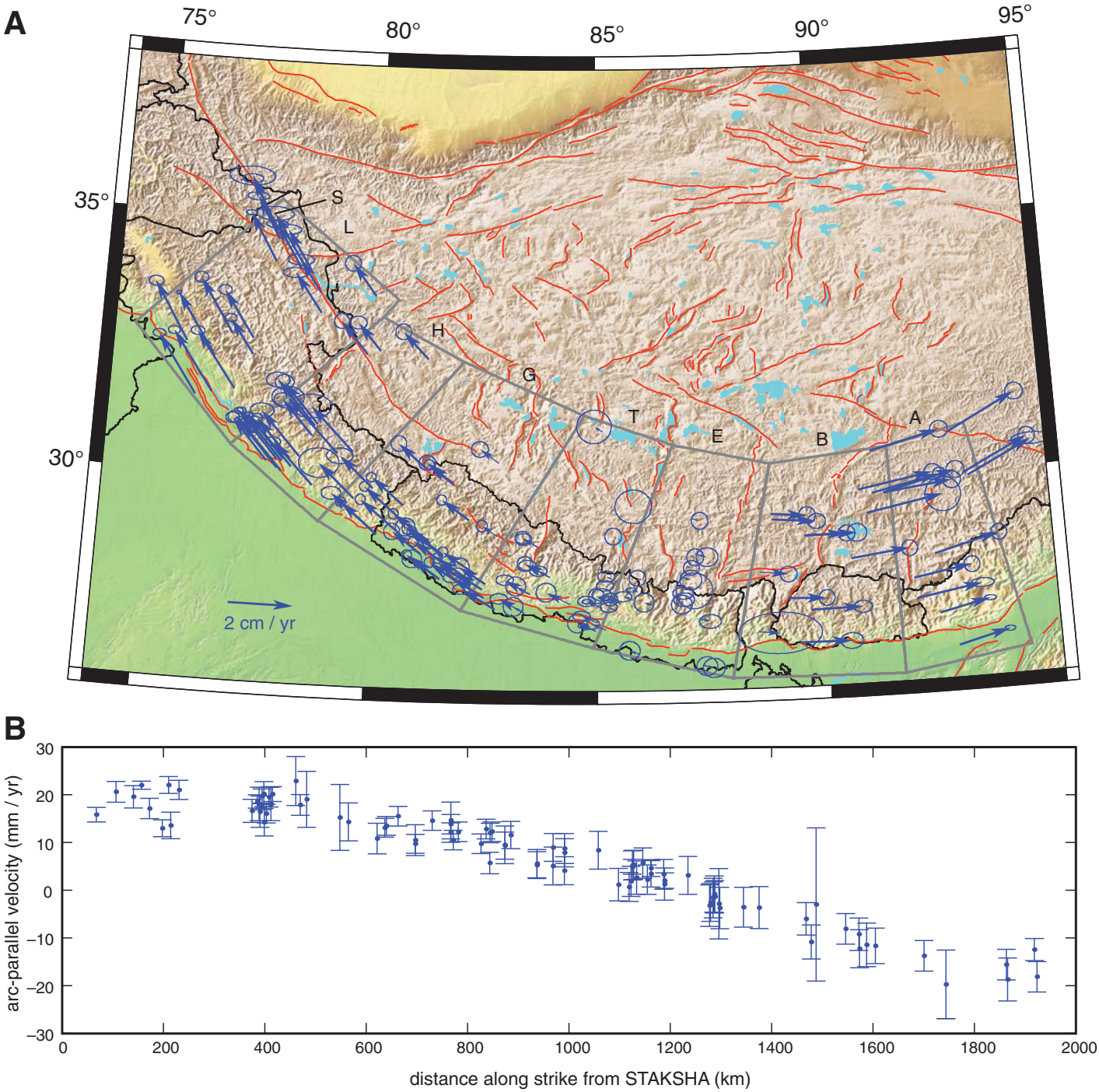

Figure 7. (A) Arc-parallel component of global positioning system (GPS) velocities. Gray boxes outline regions that define velocity bins: L—Ladakh; H—Himachal; G—Gurla Mandhata; T—Thakkhola; E—Everest; B—Bhutan; A—Arunachal; S—GPS site STAKSHA. (B) Arc-parallel component of GPS velocities from within the Himalayan arc (i.e., between the Main Frontal thrust and Karakoram fault–Indus-Yarlung suture zone) plotted as a function of distance along strike from GPS site STAKSHA. Clockwise velocities are defined as positive. The uniform velocity gradient between 400 and 1400 km along strike indicates that arc-parallel extension is uniformly distributed throughout much of the Himalaya.

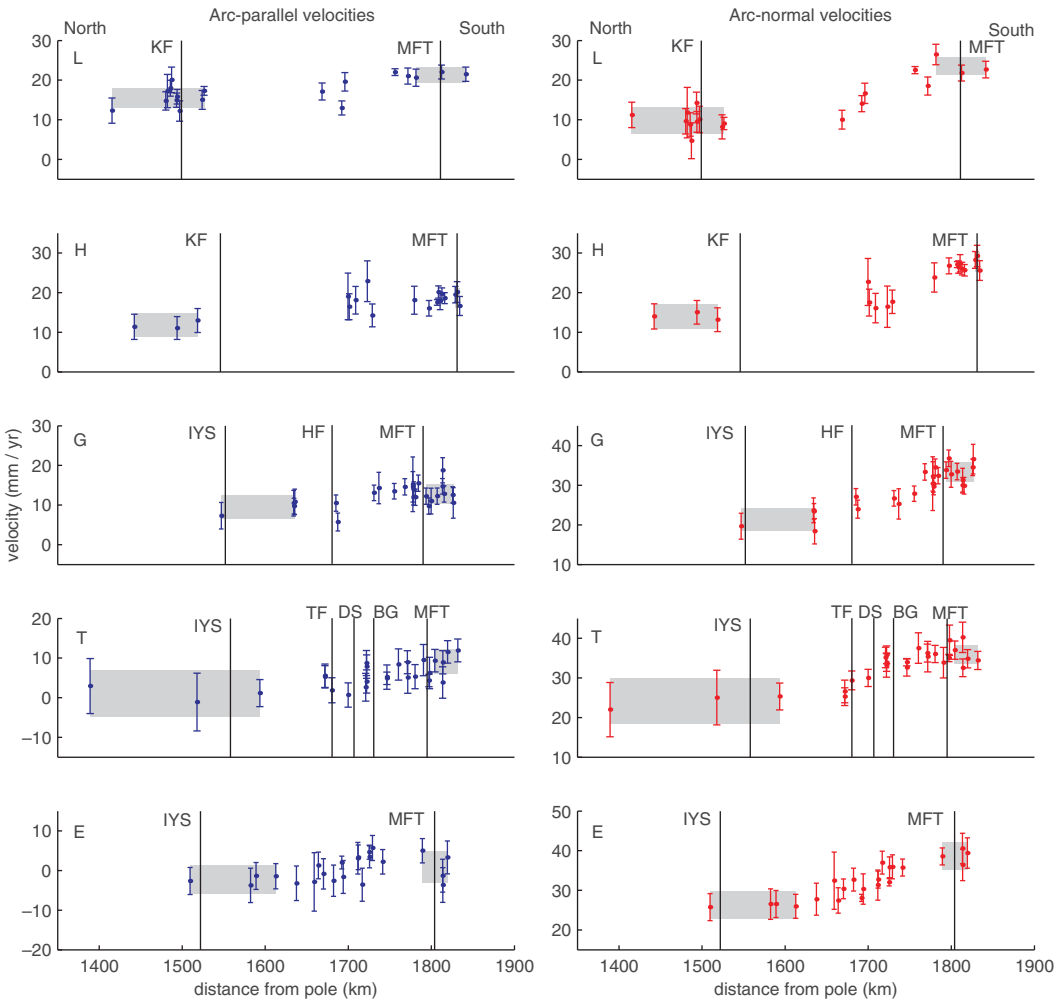

Figure 8. Arc-normal profiles of arc-parallel and arc-normal components of global positioning system (GPS) velocities for the western and central Himalayan regions shown in Figures 5 and 8. Velocities are plotted by the distance from the pole to the Himalayan arc of Bendick and Bilham (2001) at 41.4°N, 91.6°E. Positive arc-parallel velocities indicate clockwise (west- or northwest-directed) motion; increasing velocities with increasing radial distances indicate dextral shear across the arc. Positive arc-normal velocities indicate motion toward the pole; increasing velocities with increasing radial distances indicate shortening across the arc. Gray rectangles indicate the GPS sites used in the calculations of arc-normal convergence and arc-parallel shear discussed in the text. The heights of the rectangles correspond to their associated error, with the mean value in the center of the rectangle. Regions: L—Ladakh; H—Himachal; G—Gurla Mandhata; T—Thakkhola; E—Everest. KF—Karakoram fault; IYS—Indus-Yarlung suture zone; MFT—Main Frontal thrust; HF—Humla fault; TF—Tibrikot fault; DS—Dhaulagiri Southwest fault; BG—Bari Gad fault.

foreland are subtracted from the mean velocities of several sites in the interior of Tibet. This gives estimates of the amount of shear strain (positive values are right lateral) and convergence across the arc, and highlights potential along strike-velocity gradients. These results are presented in Table 1. In general, the estimates of shear strain accumulation across the arc decrease from the northwestern Himalaya toward the center of the range, and appear to increase again in the east. The estimates of arc-normal convergence are remarkably consistent across the northwestern and central portions of the arc, though there is an increase in these rates in the eastern Himalaya. However, this area seems to be undergoing clockwise vertical-axis rotation about the eastern syntaxis with little internal strain (Allmendinger et al., 2007). Therefore, the rates calculated for the eastern two regions may simply reflect the effects of vector projections of this rotational velocity field, and not shear strain or shortening across the range; for this reason, the results from these regions are not taken into account when evaluating deformational models, though they are given for completeness.

TABLE 1. ARC-PARALLEL SHEAR AND ARC-NORMAL SHORTENING RATES FOR THE GEODETIC REGIONS ALONG THE HIMALAYAN ARC

Region	Arc-parallel shear (mm yr^{-1})	Error (1 σ, mm yr^{-1})	Arc-normal shortening (mm yr^{-1})	Error (1 σ, mm yr^{-1})
Ladakh	6.0	4.4	13.7	5.6
Himachal	8.0	4.5	13.6	5.5
Gurla Mandhata	3.2	5.4	11.9	5.4
Thakkhola	8.1	8.9	11.7	8.0
Everest	3.1	7.5	12.5	6.9
Bhutan	7.9	7.2	16.1	6.1
Arunachal	6.8	5.4	24.1	4.1

Note: Rates calculated from the velocity profiles shown in Figure 8.

The transects across the arc (Fig. 8; Table 1) show that arc-parallel shear is dextral throughout the arc and statistically different than zero at the 68% confidence level only in the northwestern Himalaya. The rates of shear strain accumulation, ~6.5 ± 4.5 mm yr^{-1} (1 σ) for the Ladakh and Himachal regions, are similar to the rates of longer-term Quaternary slip along the KF from offset Quaternary glacial moraines and debris flows (Brown et al., 2002; Chevalier et al., 2005). However, it is interesting to note that this shear strain accumulation does not appear to be localized on the KF (Jade et al., 2004). The Gurla Mandhata and Everest regions

show about half the arc-parallel shear strain accumulation in comparison to the northwest regions, albeit with significantly larger errors. The Thakkhola region has the highest rate of shear strain accumulation, though that rate is still less than the 1 σ uncertainty; this error is primarily due to the large uncertainty in the velocities at remote sites in the interior of Tibet.

Though the extant geodetic sites are not positioned so that a good estimate of slip rate along the Tibrikot fault can be made (Fig. 9), the site DLP0 is located ~2 km south of the fault (between the Tibrikot and Dhaulagiri Southwest faults) and has an arc-parallel velocity of 5.71 ± 2.25 mm yr^{-1}, and the site JML0 is located ~10 km south of the Humla fault (the along-strike continuation of the Tibrikot fault) ~70 km west, and has an arc-parallel velocity of 10.50 ± 2.05 mm yr^{-1}. The next site to the south-southwest (directly toward the foreland), of DLP0 is MUL0, ~90 km away, with an arc-parallel velocity of 11.99 ± 2.05 mm yr^{-1}. While these data are certainly not sufficient to effectively bracket slip rates on the Tibrikot fault, if this velocity gradient represents half of the strain accumulation across the fault (e.g., Savage and Burford, 1973) it suggests that the Humla-Tibrikot system accumulates shear strain at several millimeters per year, similar to rates on the KF. The across-arc, arc-parallel velocity profiles in Figure 8 also suggest that all of the arc-parallel shear strain in that sector of the Himalaya is accumulating on the Humla, Tibrikot, Dhalagiri Southwest, and Bari Gad faults. This is a good indication that KF slip is transferred into the Himalaya instead of continuing along the IYS.

The arc-normal velocities vary along the Himalayan arc from ~10 to ~35 mm yr^{-1} (Figs. 8 and 10). The highest velocities are where convergence between India and the Himalaya is arc normal. However, despite the threefold variation in the velocities, the rates of convergence between geodetic sites in the Himalayan foreland and south Tibet remain remarkably consistent at ~12 mm yr^{-1} in the northwestern and central Himalaya (Fig. 8). This estimate is lower than many estimates from geology (e.g., Lavé and Avouac, 2000) and early geodesy (e.g., Larson et al., 1999), but similar to some more recent geodetic studies (e.g., Chen et al., 2004b; cf. Bettinelli et al., 2006). The along-strike consistency of the arc-normal convergence rate may indicate a dynamic equilibrium between shortening and crustal thickening in the Himalaya and extension and translation within the Tibetan Plateau.

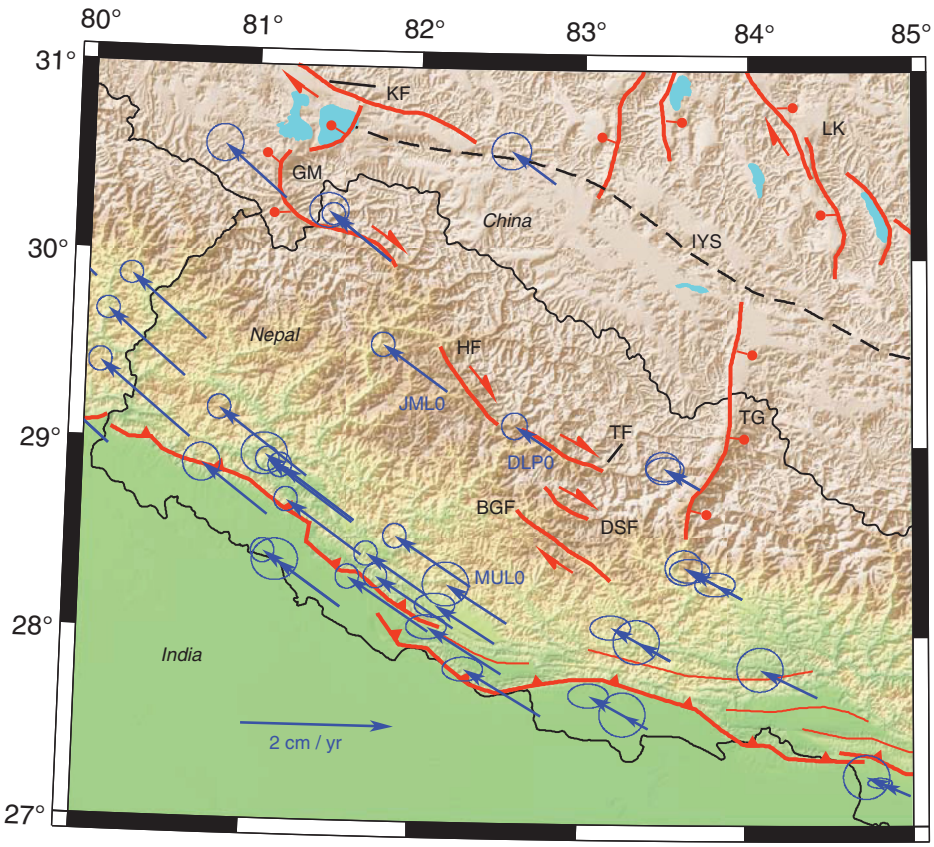

Figure 9. Active structures and arc-parallel global positioning system (GPS) velocities in western Nepal and surrounding areas. JML0, DLP0, and MUL0 are GPS sites discussed in the text. BGF—Bari Gad fault; DSF—Dhaulagiri Southwest fault; TF—Tibrikot fault; HF—Humla fault; TG—Thakkhola graben; GM—Gurla Mandhata; IYS—Indus-Yarlung suture; KF—Karakoram fault; LK—Lopukangri rift.

DISCUSSION

Evaluation of Deformational Models

We use our geodetic results and geologic observations from the literature to evaluate models of Himalayan and south Tibetan deformation by addressing the specific predictions for each model mentioned here.

The lateral extrusion model as applied to Tibet predicts that there will be high rates and magnitudes of slip along the KF, which continues along the IYS accommodating the eastward escape of Tibet. Previous geologic observations (Searle, 1991; Searle et al., 1998; Murphy et al., 2000; Phillips et al., 2004; Robinson, 2009) show a decrease in displacement magnitude along the KF to the southeast. Furthermore, in Murphy and Copeland (2005), Murphy et al. (2010), and this study, it is suggested that the majority of slip along the KF is transferred south into the Himalaya via the Gurla Mandhata–Humla fault system and continues southeast along the Tibrikot fault. Exactly how slip is transferred to the southeast from the Tibrikot fault is unknown. One possibility is that the Tibrikot fault links up with either the faults bounding the Thakkhola graben or the Dhaulagiri Southwest and Bari Gad faults. Our geodetic analysis shows that slip rates along the KF are much less than early estimates of several centimeters per year, and are not statistically different from zero along the IYS, though the errors in the dextral shear accumulation rates across the central Himalaya are large enough to allow for low (<1 cm yr^{-1}) slip along the IYS. However, the lack of seismicity indicative of right-slip faulting on the IYS and the uninterrupted rifting across the IYS into the central Himalaya (Murphy et al., 2010) strongly suggest that the IYS is not currently an active right-slip shear zone, and has not been at least since the inception of rifting in the region. The observations of an eastward increase in clockwise rotation observed in paleomagnetic data of Schill et al. (2004) in the hanging wall of the South Tibetan detachment in the north-central Himalaya may be related to faulting on of the South Tibetan detachment, as the timing constraints on those data

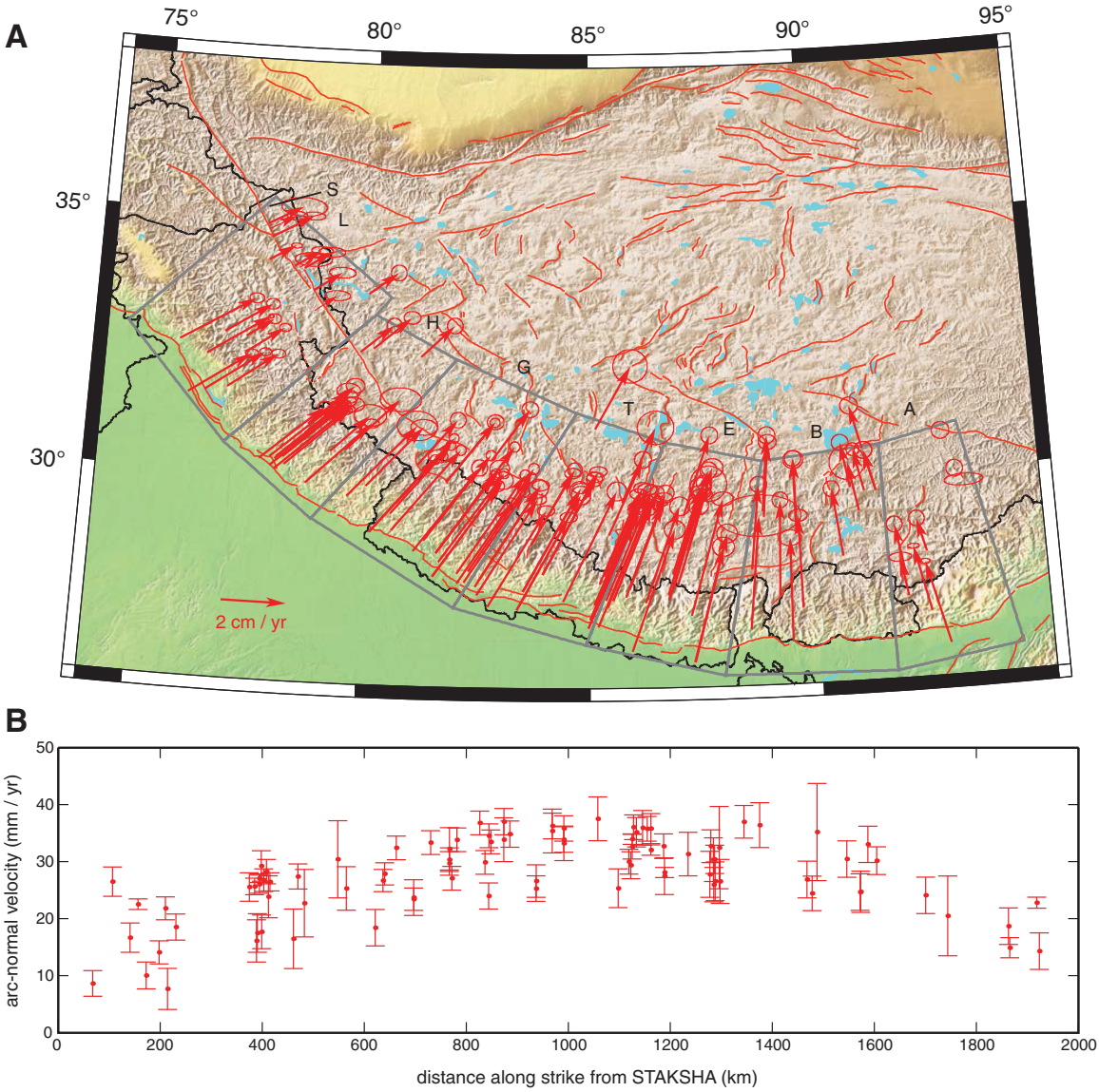

Figure 10. (A) Arc-normal component of global positioning system (GPS) velocities. Gray boxes outline regions that define velocity bins: L—Ladakh; H—Himachal; G—Gurla Mandhata; T—Thakkhola; E—Everest; B—Bhutan; A—Arunachal. S—GPS site STAKSHA. (B) Arc-normal component of GPS velocities from within the Himalayan arc (i.e., between the Main Frontal thrust and Karakoram fault–Indus-Yarlung suture zone) plotted as a function of distance along strike from GPS site STAKSHA (34.82°N, 77.52°E). Velocities directed toward the pole of Bendick and Bilham (2001) are defined as positive.

are insufficient to bracket them as post–South Tibetan detachment faulting. Furthermore, the eastward increase of clockwise rotation suggested by these data is inconsistent with through-going dextral shear on the IYS, which would produce a consistent amount of rotation along the structure. Therefore, the compiled observations do not favor it as a major active structure in regional kinematics.

The oroclinal bending model predicts that rotation of the Himalayan orocline will result in (1) east-west contraction in Tibet, (2) outer arc-parallel extension (i.e., in the frontal Himalaya), which decreases to zero along the midline of the orocline, and contraction in the interior, and possibly (3) sinistral arc-parallel strike-slip faulting in the western orogen and dextral arc-parallel strike-slip faulting in the eastern orogen. Prediction 1 is not supported by either geodetic or geologic observations, which clearly show active and well-developed east-west rifting in the Lhasa block, which in the central part of the range propagates into the Himalayan arc. Prediction 2 is partially met, as there is ample evidence for arc-parallel extension in the range; however, a switch to a contractional regime in the inner arc similar to that observed in the hinge zone of folds is not observed. Prediction 3 is also not supported by geologic or geodetic evidence, which indicates arc-parallel strike-slip faulting with slip sense opposite of that predicted. Therefore the oroclinal bending model is not supported by this study. The clockwise paleomagnetic rotations in the northwestern Indian Himalaya must be explained through other models.

The radial spreading model as applied to the Himalaya predicts that (1) the Himalayan arc will undergo arc-parallel extension, (2) the arc will move south with respect to stable Eurasia and the interior of Tibet, and (3) arc-parallel strike-slip faulting is possible. We see that prediction 1 is confirmed by both geologic and geodetic observations. Prediction 2, however, is not supported by either geologic or geodetic observations; in fact, the opposite is observed: the Himalayan arc is moving north with respect to both Eurasia and the interior of Tibet. This is not immediately apparent in the geodetic studies that utilized an India-fixed reference frame, because they either do not extend far enough north so that the north-south contraction across Tibet is observable (Jade et al., 2007; Banerjee et al., 2008), or the data are too sparse for this to be apparent (Jade et al., 2004). However, the northward velocities observed near the Bangong-Nujiang suture zone (Fig. 6) are too far north of the Main Himalayan thrust to be significantly influenced by elastic effects due to locking on the Main Himalayan thrust (Bettinelli et al., 2006; cf. Feldl and Bilham, 2006). Furthermore, shortening in the direction of Indo-Eurasian relative motion continues throughout the entirety of the plateau, between the Himalaya and the rigid basins to the north, at significant (>10 mm yr^{-1}) rates (Zhang et al., 2004). This cannot be coeval with the radial, southwest- to southeast-directed extension required by the radial spreading model (Copley and McKenzie, 2007). The only geologic observations that could support prediction 2 are those describing the South Tibetan detachment system, an Early Miocene structure whose recent activity has been suggested (e.g., Hurtado et al., 2001), but active slip on this system would be inconsistent with the geodetic strain field. Prediction 3, which is not a firm requirement of the model but a modification made to incorporate geologic observations, is not inconsistent with this analysis. The geologic evidence supporting radial spreading is primarily arc-parallel extension and strike-slip faulting within the Himalaya (Murphy et al., 2002, 2009). Therefore, this study does not support radial spreading as a viable mechanism for modern Himalayan deformation.

The variably oblique convergence model for Himalayan deformation predicts (1) an increasing arc-parallel velocity gradient away from the region of purely normal Indo-Himalayan convergence in eastern Nepal, (2) arc-parallel extension of the Himalaya, and (3) increasing rates and magnitudes of Himalayan arc-parallel translation away from the central range along arc-parallel strike-slip faults. This study confirms prediction 1; arc-parallel velocities are near zero near Everest, and velocities increase toward the syntaxes. To the west, this velocity gradient is geologically expressed as extension of the Himalayan arc from the Thakkhola graben region to the northwest, bounded to the north by the KF; net slip estimates across the Karakoram (Robinson, 2009), Humla (Murphy and Copeland, 2005), and likely the Tibrikot faults increase to the northwest. This results in the observation of prediction 2, arc-parallel extension distributed throughout the Himalaya. Prediction 3 is also confirmed by this study and many others. Rates of dextral shear accumulation across the arc increase to the northwest as well, though the uncertainties are large enough that all values may be equal at the 68% confidence level. Therefore, the results of this study support the oblique convergence model for Himalayan deformation over the other models considered. These results only apply for the present deformational phase (to which all of the data discussed here apply), characterized by arc-parallel extension and translation of the Himalayan arc, which seems to have begun in the Middle Miocene, as discussed herein. In the next section we discuss the implications of variably oblique convergence as applied to the Himalaya.

Oblique Convergence and Himalayan Deformation

As the Indian plate underthrusts Tibet, it exerts a shear stress on the base of the Himalayan orogenic wedge. The orientation of this shear stress with respect to the strike of the wedge changes along strike, so that there is an increasing component of traction parallel to the wedge away from the region of normal convergence in eastern Nepal. This causes extension of the Himalayan arc. Where this convergence is oblique to the strike of the arc, the arc-parallel component induces translation of the Himalaya relative to south Tibet. In the northwest Himalaya, the extending Himalayan arc translates differentially along the KF against a relatively unextended western Lhasa block, so that the slip rates and magnitudes along the KF increase to the northwest. Slip on the KF steps to the south at Gurla Mandhata, which is interpreted to be a releasing bend having undergone several tens of kilometers of extension (Murphy et al., 2002), and continues as dextral slip along a series of en echelon faults (including the Humla, Tibrikot, and Bari Gad faults) cutting across the Nepalese Himalaya. Net slip on the Humla is estimated as 25–30 km (Murphy and Copeland, 2005). The faults to the southeast likely have less displacement (Murphy et al., 2010). The initiation of strike-slip faulting seems to be diachronous; Phillips et al. (2004) described the central KF as being active at 15 Ma, while to the southeast, the KF cannot have begun cutting the South Kailas thrust until thrusting ceased after 13 Ma (Yin et al., 1999b; Murphy et al., 2000). The Humla fault, which cuts the South Tibetan detachment system, also must have initiated after the latter's cessation (Murphy and Copeland, 2005). The Tibrikot fault must have begun cutting the Main Central thrust zone rocks after thrusting ceased, as late as 4 Ma (Harrison et al., 1997). This southeastward propagation of dextral faulting may be related to a shear stress gradient along this zone (highest in the northwest), as well as the successive southward propagation of the Himalayan active thrust front as material is accreted to the front and base of the Himalayan wedge. In the central Himalaya, both the range and the Tibetan Plateau are extending in the same general direction, and many of the rifts that accommodate this extension are common to both domains and are apparently continuous across the IYS. The rates of extension are similar to the north and to the south of the IYS zone, thus a transfer zone along the IYS is not necessary. Farther east, arc-parallel and subparallel sinistral faulting occurs, but this faulting is not as developed as in the west (Li and Yin, 2008). This transitions into clockwise rotation around the eastern Himalayan syntaxis (Allmendinger et al., 2007; Shen et al., 2005) as the Main Himalayan thrust meets the dextral, north-striking Sagaing fault, which is the boundary between the Indian and Sunda plates (Liu and Bird, 2008).

Though the Himalaya and Tibet are both actively extending, the differences in the orientation and location of the extension direction suggest that the style of extension throughout the orogen arises from two different mechanisms: (1) variably oblique convergence causes Himalayan arc-parallel extension, while (2) extension in the Tibetan Plateau likely results from a combination of excess of gravitational potential energy in Tibet (e.g., England and Houseman, 1988; Copley, 2008), compression applied to the southern Eurasia plate by the Indian plate (e.g., Vergnolle et al., 2007), and possibly widespread basal tractions (Taylor and Yin, 2009).

CONCLUSIONS

Analysis of GPS velocities in the Himalaya and southern Tibet shows that the central and northwestern Himalaya is undergoing arc-parallel extension. This extension is bound by dextral shear in the northwest, which may be accommodated on the KF. Shortening across the central and northwestern Himalaya is very consistent at ~12 mm yr^{-1}. The northward movement

of the Himalaya with respect to central Tibet and stable Eurasia, the arc-parallel extension of the Himalaya, and the lack of significant dextral slip along the IYS all suggest that arc-parallel extension and translation in the Himalaya result from variably oblique convergence between India and the Himalaya.

ACKNOWLEDGMENTS

Invaluable assistance in the field was provided by Bhim Chand. The Generic Mapping Tools (Wessel and Smith, 1988) were used in generating Figures 1, 2, 6, 7, 9, and 10. Styron thanks the authors of the publications whose geodetic data were used in this study (Zhang et al., 2004; Paul et al., 2001; Wang et al., 2001; Banerjee and Bürgmann, 2002; Jade et al., 2004, 2007; Bettinelli et al., 2006). Taylor and Murphy acknowledge support for field work from grants from the Tectonics Division of the U.S. National Science Foundation. Comments by Science Editor D. Harry, Associate Editor F. Mazzarini, and reviews by two anonymous reviewers greatly improved the manuscript.

REFERENCES CITED

Allmendinger, R.W., Reilinger, R., and Loveless, J., 2007, Strain and rotation rate from GPS in Tibet, Anatolia, and the Altiplano: Tectonics, v. 26, TC3013, doi: 10.1029/2006TC002030.

Altamimi, Z., Sillard, P., and Boucher, C., 2002, ITRF2000: A new release of the International Terrestrial Reference Frame for earth science applications: Journal of Geophysical Research, v. 107, 2214, doi: 10.1029/2001JB000561.

Armijo, R., Tapponnier, P., Mercier, J., and Tong-Lin, H., 1986, Quaternary extension in southern Tibet: Field observations and tectonic implications: Journal of Geophysical Research, v. 91, p. 13,803–13,872, doi: 10.1029/JB091iB14p13803.

Armijo, R., Tapponnier, P., and Han, T., 1989, Late Cenozoic right-lateral strike-slip faulting in southern Tibet: Journal of Geophysical Research, v. 94, p. 2787–2838, doi: 10.1029/JB094iB03p02787.

Avé Lallemant, H.G., and Oldow, J.S., 2000, Active displacement partitioning and arc-parallel extension of the Aleutian volcanic arc based on global positioning system geodesy and kinematic analysis: Geology, v. 28, p. 739–742, doi: 10.1130/0091-7613(2000)28<739:ADPAAE>2.0.CO;2.

Baltz, T., and Murphy, M.A., 2009, Structural evolution of the Thakkhola graben and implications on the architecture of the central Himalaya: Eos (Transactions, American Geophysical Union), v. 90, no. 58, fall meeting supplement, abs. T43C–2110.

Banerjee, P., and Bürgmann, R., 2002, Convergence across the northwest Himalaya from GPS measurements: Geophysical Research Letters, v. 29, 1652, 4 p., doi: 10.1029/2002GL015184.

Banerjee, P., Bürgmann, R., Nagarajan, B., and Apel, E., 2008, Intraplate deformation of the Indian subcontinent: Geophysical Research Letters, v. 35, L18301, doi: 10.1029/2008GL035468.

Beaumont, C., Jamieson, R.A., Nguyen, M.H., and Medvedev, S., 2004, Crustal channel flows: 1. Numerical models with applications to the tectonics of the Himalayan-Tibetan orogen: Journal of Geophysical Research, v. 109, B06406, doi: 10.1029/2003JB002809.

Bendick, R., and Bilham, R., 2001, How perfect is the Himalayan arc?: Geology, v. 29, p. 791–794, doi: 10.1130/0091-7613(2001)029<0791:HPITHA>2.0.CO;2.

Bendick, R., Bilham, R., Khan, M.A., and Khan, S.F., 2007, Slip on an active wedge thrust from geodetic observations of the 8 October 2005 Kashmir earthquake: Geology, v. 35, p. 267–270, doi: 10.1130/G23158A.1.

Bettinelli, P., Avouac, J.-P., Flouzat, M., Jouanne, F., Bollinger, L., Willis, P., and Chitrakar, G., 2006, Plate motion of India and interseismic strain in the Nepal Himalaya from GPS and DORIS Measurements: Journal of Geodesy, v. 80, p. 567–589, doi: 10.1007/s00190-006-0030-3.

Bird, P., 1991, Lateral extrusion of lower crust from under high topography, in the isostatic limit: Journal of Geophysical Research, v. 96, p. 10,275–10,286, doi: 10.1029/91JB00370.

Bordet, P., Colchen, M., Krummenacher, D., Le Fort, P., Mouterde, R., and Remy, M., 1971, Recherches géologiques dans l'Himalaya du Népal, région de la Thakkhola: Paris, Centre National de la Recherche Scientifique, 279 p.

Brown, E.T., Bendick, R., Bourlès, D.L., Gaur, V., Molnar, P., Raisbeck, G.M., and Yiou, F., 2002, Slip rates of the Karakorum fault, Ladakh, India, determined using cosmic ray exposure dating of debris flows and moraines: Journal of Geophysical Research, v. 107, no. B9, 2192, 13 p., doi: 10.1029/2000JB000100.

Chen, Q.Z., Freymueller, J.T., Wang, Q., Yang, Z.Q., Xu, C.J., and Liu, J.N., 2004a, A deforming block model for the present-day tectonics of Tibet: Journal of Geophysical Research, v. 109, B09401, doi: 10.1029/2002JB002350.

Chen, Q.Z., Freymueller, J.T., Yang, Z.Q., Xu, C.J., Jiang, W.P., Wang, Q., and Liu, J.N., 2004b, Spatially variable extension in southern Tibet based on GPS measurements: Journal of Geophysical Research, v. 109, B01403, doi: 10.1029/2002JB002151.

Chevalier, M.-L., Ryerson, F.J., Tapponnier, P., Finkel, R.C., Van Der Woerd, J., Haibing, L., and Qing, L., 2005, Slip-rate measurements on the Karakorum fault may imply secular variations in fault motion: Science, v. 307, p. 411–414, doi: 10.1126/science.1105466.

Clark, M.K., and Bilham, R., 2008, Miocene rise of the Shillong Plateau and the beginning of the end for the eastern Himalaya: Earth and Planetary Science Letters, v. 269, p. 337–350, doi: 10.1016/j.epsl.2008.01.045.

Clark, R.J., 2005, Structural constraints on the exhumation of the Tso Morari Dome, NW Himalaya [M.S. thesis]: Cambridge, Massachusetts Institute of Technology, 52 p.

Cogan, M.J., Nelson, K.D., Kidd, W.S.F., Wu, C., and Project, I.T., 1998, Shallow structure of the Yadong-Gulu rift, southern Tibet, from refraction analysis of Project INDEPTH common midpoint data: Tectonics, v. 17, p. 46–61, doi: 10.1029/97TC03025.

Colchen, M., Le Fort, P., and Pêcher, A., 1986, Annapurna–Manaslu–Ganesh Himal: Paris, Centre National de laRecherche Scientifique, 136 p.

Cook, K.L., and Royden, L.H., 2008, The role of crustal strength variations in shaping orogenic plateaus, with application to Tibet: Journal of Geophysical Research, v. 113, B08407, doi: 10.1029/2007JB005457.

Copley, A., 2008, Kinematics and dynamics of the southeastern margin of the Tibetan Plateau: Geophysical Journal International, v. 174, p. 1081–1100, doi: 10.1111/j.1365-246X.2008.03853.x.

Copley, A., and McKenzie, D., 2007, Models of crustal flow in the India-Asia collision zone: Geophysical Journal International, v. 169, p. 683–698, doi: 10.1111/j.1365-246X.2007.03343.x.

Dewane, T., Stockli, D., Hager, C., Taylor, M., Ding, L., Lee, J., and Wallis, S., 2006, Timing of Cenozoic E-W extension in the Tangra Yum Co-Kung Co Rift, south-central Tibet: Eos (Transactions, American Geophysical Union), v. 87, no. 52, fall meeting supplement, abs. T34C–04.

Dewey, J.F., 1988, Extensional collapse of orogens: Tectonics, v. 7, p. 1123–1139, doi: 10.1029/TC007i006p01123.

Drukpa, D., Velasco, A., and Doser, D., 2006, Seismicity in the Kingdom of Bhutan (1937–2003): Evidence for crustal transcurrent deformation: Journal of Geophysical Research, v. 111, B06301, doi: 10.1029/2004JB003087.

England, P.C., and Houseman, G.A., 1988, The mechanics of the Tibetan Plateau: Royal Society of London Philosophical Transactions, ser. A, v. 326, p. 301–319, doi: 10.1098/rsta.1988.0089.

Epard, J.-L., and Steck, A., 2004, The Eastern prolongation of the Zanskar Shear Zone (Western Himalaya): Eclogae Geologicae Helvetiae, v. 97, p. 193–212, doi: 10.1007/s00015-004-1116-7.

Epard, J.-L., and Steck, A., 2008, Structural development of the Tso Morari ultra-high pressure nappe of the Ladakh Himalaya: Tectonophysics, v. 451, p. 242–264, doi: 10.1016/j.tecto.2007.11.050.

Feldl, N., and Bilham, R., 2006, Great Himalayan earthquakes and the Tibetan plateau: Nature, v. 444, p. 165–170, doi: 10.1038/nature05199.

Gan, W., Zhang, P., Shen, Z., Niu, Z., Wang, M., Wan, Y., Zhou, D., and Cheng, J., 2007, Present-day crustal motion within the Tibetan Plateau inferred from GPS measurements: Journal of Geophysical Research, v. 112, B08416, doi: 10.1029/2005JB004120.

Garzione, C.N., DeCelles, P.G., Hodkinson, D.G., Ojha, T.P., and Upreti, B.N., 2003, East-west extension and Miocene environmental change in the southern Tibetan plateau: Thakkhola graben, central Nepal: Geological Society of America Bulletin, v. 115, p. 3–20, doi: 10.1130/0016-7606(2003)115<0003:EWEAME>2.0.CO;2.

Godin, L., Parrish, R.R., Brown, R.L., and Hodges, K.V., 2001, Crustal thickening leading to exhumation of the Himalayan metamorphic core of central Nepal: Insight from U-Pb geochronology and $^{40}Ar/^{39}Ar$ thermochronology: Tectonics, v. 20, p. 729–747, doi: 10.1029/2000TC001204.

Hager, C., Stockli, D., Dewane, T., Ding, L., Taylor, M., and Lee, J., 2006, Episodic Mio-Pliocene rifting in south-central Tibet. Thermochronometric constraints from the Xainza rift: Eos (Transactions, American Geophysical Union), v. 87, no. 52, fall meeting supplement, abs. T34C–02.

Harrison, T.M., Ryerson, F.J., LeFort, P., Yin, A., Lovera, O.M., and Catlos, E.J., 1997, A Late Miocene–Pliocene origin for the Central Himalayan inverted metamorphism: Earth and Planetary Science Letters, v. 146, p. E1–E7, doi: 10.1016/S0012-821X(96)00215-4.

Hodges, K.V., Parrish, R.R., and Searle, M.P., 1996, Tectonic evolution of the central Annapurna Range, Nepalese Himalayas: Tectonics, v. 15, p. 1264–1291, doi: 10.1029/96TC01791.

Hodges, K.V., Wobus, C., Ruhl, K., Schildgen, T., and Whipple, K., 2004, Quaternary deformation, river steepening, and heavy precipitation at the front of the Higher Himalayan ranges: Earth and Planetary Science Letters, v. 220, p. 379–389, doi: 10.1016/S0012-821X(04)00063-9.

Hurtado, J., Hodges, K., and Whipple, K., 2001, Neotectonics of the Thakkhola graben and implications for recent activity on the South Tibetan fault system in the central Nepal Himalaya: Geological Society of America Bulletin, v. 113, p. 222–240, doi: 10.1130/0016-7606(2001)113<0222:NOTTGA>2.0.CO;2.

Jade, S., Bhatt, B., Yang, Z., Bendick, R., Gaur, V., Molnar, P., Anand, M., and Kumar, D., 2004, GPS measurements from the Ladakh Himalaya, India: Preliminary tests of plate-like or continuous deformation in Tibet: Geological Society of America Bulletin, v. 116, p. 1385–1391, doi: 10.1130/B25357.1.

Jade, S., Mukul, M., Bhattacharyya, A., Vijayan, M., Jaganathan, S., Kumar, A., Tiwari, R., Kalita, S., and Sahu, S., 2007, Estimates of interseismic deformation in northeast India from GPS measurements: Earth and Planetary Science Letters, v. 263, p. 221–234, doi: 10.1016/j.epsl.2007.08.031.

Jessup, M., Newell, D., Cottle, J., Berger, A., and Spotila, J., 2008, Orogen-parallel extension and exhumation enhanced by denudation in the trans-Himalayan Arun River gorge, Ama Drime Massif, Tibet-Nepal: Geology, v. 36, p. 587–590, doi: 10.1130/G24722A.1.

Jouanne, F., Mugnier, J.L., Pandey, M.R., Gamond, J.F., Le Fort, P., Serrurier, L., Vigny, C., and Avouac, J.P., 1999, Oblique convergence in the Himalayas of western Nepal deduced from preliminary results of GPS measurements: Geophysical Research Letters, v. 26, p. 1933–1936, doi: 10.1029/1999GL900416.

Kali, E., Leloup, P.H., Arnaud, N., Mahéo, G., Liu, D., Boutonnet, E., Van der Woerd, J., Liu, X., Liu-Zeng, J., and Li, H., 2010, Exhumation history of the deepest central Himalayan rocks, Ama Drime range: Key pressure-temperature-deformation-time constraints on orogenic models: Tectonics, v. 29, TC2014, doi: 10.1029/2009TC002551.

Kapp, P., and Guynn, J.H., 2004, Indian punch rifts Tibet: Geology, v. 32, p. 993–996, doi: 10.1130/G20689.1.

Klootwijk, C.T., Conaghan, P.J., and Powell, C.M., 1985, The Himalayan Arc—Large-scale continental subduction, oroclinal bending and back-arc spreading: Earth and Planetary Science Letters, v. 75, p. 167–183, doi: 10.1016/0012-821X(85)90099-8.

Lacassin, R., Valli, F., Arnaud, N., Leloup, P.H., Paquette, J.L., Haibing, L., Tapponnier, P., Chevalier, M.-L., Guillot, S., Mahéo, G., and Zhiqin, X., 2004, Large-scale geometry, offset and kinematic evolution of the Karakorum fault, Tibet: Earth and Planetary Science Letters, v. 219, p. 255–269, doi: 10.1016/S0012-821X(04)00006-8.

Langille, J.M., Jessup, M.J., Cottle, J.M., Newell, D., and Seward, G., 2010, Kinematic evolution of the Ama Drime detachment: Insight into orogen-parallel extension and exhumation of the Ama Drime Massif, Tibet-Nepal: Journal of Structural Geology, v. 32, p. 900–919, doi: 10.1016/j.jsg.2010.04.005.

Larson, K.M., Bürgmann, R., Bilham, R., and Freymueller, J.T., 1999, Kinematics of the India-Eurasia collision zone from GPS measurements: Journal of Geophysical Research, v. 104, no. B1, p. 1077–1093, doi: 10.1029/1998JB900043.

Lavé, J., and Avouac, J.P., 2000, Active folding of fluvial terraces across the Siwaliks Hills, Himalayas of central Nepal: Journal of Geophysical Research, v. 105, no. B3, p. 5735–5770, doi: 10.1029/1999JB900292.

Lee, J., Hager, C., Wallis, S.R., Stockli, D.F., Whitehouse, M.J., Aoya, M., and Wang, Y., 2011, Middle to late Miocene extremely rapid exhumation and thermal re-equilibriation in the Kung Co rift, southern Tibet: Tectonics, doi: 10.1029/2010TC002745, (in press).

Li, D., and Yin, A., 2008, Orogen-parallel, active left-slip faults in the Eastern Himalaya: Implications for the growth mechanism of the Himalayan Arc: Earth and Planetary Science Letters, v. 274, p. 258–267, doi: 10.1016/j.epsl.2008.07.043.

Liu, Z., and Bird, P., 2008, Kinematic modelling of neotectonics in the Persia-Tibet-Burma orogen: Geophysical Journal International, v. 172, p. 779–797, doi: 10.1111/j.1365-246X.2007.03640.x.

Mahéo, G., Leloup, P.H., Valli, F., Lacassin, R., Arnaud, N., Paquette, J.L., Fernandez, A., Haibing, L., Farley, K.A., and Tapponnier, P., 2007, Post 4 Ma initiation of normal faulting in southern Tibet. Constraints from the Kung Co half graben: Earth and Planetary Science Letters, v. 256, p. 233–243, doi: 10.1016/j.epsl.2007.01.029.

McCaffrey, R., 1992, Oblique plate convergence, slip vectors, and forearc deformation: Journal of Geophysical Research, v. 97, p. 8905–8915, doi: 10.1029/92JB00483.

McCaffrey, R., and Nábelek, J., 1998, Role of oblique convergence in the active deformation of the Himalayas and southern Tibet plateau: Geology, v. 26, p. 691–694, doi: 10.1130/0091-7613(1998)026<0691:ROOCIT>2.3.CO;2.

Meade, B., 2007, Present-day kinematics at the India-Asia collision zone: Geology, v. 35, p. 81–84, doi: 10.1130/G22924A.1.

Métivier, F., Gaudemer, Y., Tapponnier, P., and Meyer, B., 1998, Northeastward growth of the Tibet plateau deduced from balanced reconstruction of two depositional areas: The Qiadam and Hexi Corridor basins, China: Tectonics, v. 17, p. 823–842, doi: 10.1029/98TC02764.

Molnar, P., and Lyon-Caen, H., 1989, Fault plane solutions of earthquakes and active tectonics of the Tibetan Plateau and its margins: Geophysical Journal International, v. 99, p. 123–153, doi: 10.1111/j.1365-246X.1989.tb02020.x.

Molnar, P., England, P., and Martinod, J., 1993, Mantle dynamics, uplift of the Tibetan Plateau, and the Indian Monsoon: Reviews of Geophysics, v. 31, p. 357–396, doi: 10.1029/93RG02030.

Murphy, M.A., and Burgess, W.P., 2006, Geometry, kinematics, and landscape characteristics of an active transtension zone, Karakoram fault system, southwest Tibet: Journal of Structural Geology, v. 28, p. 268–283, doi: 10.1016/j.jsg.2005.10.009.

Murphy, M.A., and Copeland, P., 2005, Transtensional deformation in the central Himalaya and its role in accommodating growth of the Himalayan orogen: Tectonics, v. 24, TC4012, doi: 10.1029/2004TC001659.

Murphy, M.A., Yin, A., Kapp, P., Harrison, T.M., Lin, D., and Guo, J.H., 2000, Southward propagation of the Karakoram fault system, southwest Tibet: Timing and magnitude of slip: Geology, v. 28, p. 451–454, doi: 10.1130/0091-7613(2000)28<451:SPOTKF>2.0.CO;2.

Murphy, M., Yin, A., Kapp, P., Harrison, T., Manning, C., Ryerson, F., Lin, D., and Jinghui, G., 2002, Structural evolution of the Gurla Mandhata detachment system, southwest Tibet: Implications for the eastward extent of the Karakoram fault system: Geological Society of America Bulletin, v. 114, p. 428–447, doi: 10.1130/0016-7606(2002)114<0428:SEOTGM>2.0.CO;2.

Murphy, M.A., Saylor, J.E., and Ling, D., 2009, Landscape evolution of southwest Tibet based on integrated paleoelevation reconstructions and structural history: Earth and Planetary Science Letters, v. 282, p. 1–9, doi: 10.1016/j.epsl.2009.01.006.

Murphy, M.A., Sanchez, V., and Taylor, M.H., 2010, Syncollisional extension along the India-Asia suture zone, south-central Tibet: Implications for crustal deformation of Tibet: Earth and Planetary Science Letters, v. 290, p. 233–243, doi: 10.1016/j.epsl.2009.11.046.

Nakata, T., 1989, Active faults of the Himalaya of India and Nepal: Tectonics of the western Himalayas, *in* Malinconico, L.L., Jr., and Lillie, R., eds., Tectonics of the Western Himalayas: Geological Society of America Special Paper 232, p. 243–264.

Paul, J., Bürgmann, R., Gaur, V.K., Bilham, R., Larson, K.M., Ananda, M.B., Jade, S., Mukal, M., Anupama, T.S., Satyal, G., and Kumar, D., 2001, The motion and active deformation of India: Geophysical Research Letters, v. 28, p. 647–651, doi: 10.1029/2000GL011832.

Peltzer, G., and Tapponnier, P., 1988, Formation and evolution of strike-slip faults, rifts, and basins during the India-Asia collision—An experimental approach: Journal of Geophysical Research, v. 93, p. 15,085–15,117, doi: 10.1029/JB093iB12p15085.

Phillips, R.J., Parrish, R.R., and Searle, M.P., 2004, Age constraints on ductile deformation and long-term slip rates along the Karakoram fault zone, Ladakh: Earth and Planetary Science Letters, v. 226, p. 305–319, doi: 10.1016/j.epsl.2004.07.037.

Ratschbacher, L., Frisch, W., Liu, G., and Chen, C., 1994, Distributed deformation in southern and western Tibet during and after the India-Asia collision: Journal of Geophysical Research, v. 99, no. B10, p. 19,917–19,945, doi: 10.1029/94JB00932.

Robinson, A.C., 2009, Geologic offsets across the northern Karakorum fault: Implications for its role and terrane correlations in the western Himalayan-Tibetan orogen: Earth and Planetary Science Letters, v. 279, p. 123–130, doi: 10.1016/j.epsl.2008.12.039.

Royden, L.H., Burchfiel, B.C., King, R.W., Wang, E., Chen, Z.L., Shen, F., and Liu, Y.P., 1997, Surface deformation and lower crustal fl ow in eastern Tibet: Science, v. 276, p. 788–790, doi: 10.1126/science.276.5313.788.

Savage, J., and Burford, R., 1973, Geodetic determination of relative plate motion in central California: Journal of Geophysical Research, v. 78, p. 832–845, doi: 10.1029/JB078i005p00832.

Schill, E., Appel, E., Zeh, O., Singh, V., and Gautam, P., 2001, Coupling of late-orogenic tectonics and secondary pyrrhotite remanences: Towards a separation of different rotation processes and quantification of rotational underthrusting in the western Himalaya (northern India): Tectonophysics, v. 337, p. 1–21, doi: 10.1016/S0040-1951(01)00113-5.

Schill, E., Crouzet, C., Gautam, P., Singh, V.K., and Appel, E., 2002, Where did rotational shortening occur in the Himalayas? Inferences from palaeomagnetic remagnetisations: Earth and Planetary Science Letters, v. 203, p. 45–57, doi: 10.1016/S0012-821X(02)00842-7.

Schill, E., Appel, E., Crouzet, C., Gautam, P., Wehland, F., Staiger, M., 2004, Oroclinal bending versus regional significant clockwise rotations in the Hamalayan arc—Constraints from secondary pyrrhotite remanences, *in* Sussman, A.J., Weil, A.B., eds., Orogenic Curvature: Integrating Paleomagnetic and Structural Analyses: Geological Society of America Special Paper 383, p. 73–85, doi: 10.1130/0-8137-2383-3(2004)383[73:OBVRSC]2.0.CO;2.

Searle, M., 1991, Geology and tectonics of the Karakoram Mountains: New York, John Wiley & Sons Inc, 358 p.

Searle, M.P., 1996, Geological evidence against large-scale pre-Holocene offsets along the Karakoram fault: Implications for the limited extrusion of the Tibetan Plateau: Tectonics, v. 15, p. 171–186, doi: 10.1029/95TC01693.

Searle, M., 2010, Low-angle normal faults in the compressional Himalayan orogen: Evidence from the Annapurna-Dhaulagiri Himalaya, Nepal: Geosphere, v. 6, p. 296–315, doi: 10.1130/GES00549.1.

Searle, M.P., and Godin, L., 2003, The South Tibetan detachment and the Manaslu leucogranite: A structural re-interpretation and restoration of the Annapurna-Manaslu Himalaya, Nepal: Journal of Geology, v. 111, p. 505–523, doi: 10.1086/376763.

Searle, M.P., Weinberg, R.F., and Dunlap, W.J., 1998, Transpressional tectonics along the Karakoram fault zone, northern Ladakh: Constraints on Tibetan extrusion, *in* Holdsworth, R.E., et al., eds., Continental transpressional and transtensional tectonics. Geological Society of London Special Publication 135, p. 307–326, doi: 10.1144/GSL.SP.1998.135.01.20.

Seeber, L., and Pêcher, A., 1998, Strain partitioning along the Himalayan arc and the Nanga Parbat antiform: Geology, v. 26, p. 791–794, doi: 10.1130/0091-7613(1998)026<0791:SPATHA>2.3.CO;2.

Shen, Z., Lu, J., Wang, M., and Bürgmann, R., 2005, Contemporary crustal deformation around the southeast borderland of the Tibetan plateau: Journal of Geophysical Research, v. 110, B11409, 17 p., doi: 10.1029/2004JB003421.

Steck, A., Epard, J.-L., Vannay, J.-C., Hunziker, J., Girard, M., Morard, A., and Robyr, M., 1998, Geological transect across the Tso Morari and Spiti areas: The nappe structures of the Tethys Himalaya: Eclogae Geologicae Helvetiae, v. 91, p. 103–121.

Styron, R., Taylor, M., and Murphy, M., 2009, Himalayan orogen-parallel extension from GPS geodesy and structural geology: 5th International Symposium on Tibetan Plateau– 24th Himalaya-Karakorum-Tibet Workshop, Beijing, China, p. 11–14.

Styron, R., Taylor, M., and Okoronkwo, K., 2010, Database of active structures from the Indo-Asian Collision: Eos (Transactions, American Geophysical Union), v. 91, no. 20, doi: 10.1029/2010EO200001.

Sundell, K., Taylor, M., Stockli, D., Styron , R., Kapp, P., Liu, D., and Ding, L., 2010, Low-temperature thermochronology of the North Lunggar Rift, west-central Tibet: Geological Society of America Abstracts with Program, v. 42, no. 5, p. 664.

Tapponnier, P., Peltzer, G., Le Dain, A.Y., Armijo, R., and Cobbold, P., 1982, Propagating extrusion tectonics in Asia: New insights from simple experiments with plasticine: Geology, v. 10, p. 611–616, doi: 10.1130/0091-7613(1982)10<611:PETIAN>2.0.CO;2.

Tapponnier, P., Xu, Z.Q., Roger, F., Meyer, B., Arnaud, N., Wittlinger, G., and Yang, J.S., 2001, Oblique stepwise rise and growth of the Tibet plateau: Science, v. 294, p. 1671–1677, doi: 10.1126/science.105978.

Taylor, M., and Peltzer, G., 2006, Current slip rates on conjugate strike slip faults in central Tibet using synthetic aperture radar interferometry: Journal of Geophysical Research, v. 111, B12402, 16 p., doi: 10.1029/2005JB004014.

Taylor, M., and Yin, A., 2009, Active structures of the Himalayan-Tibetan orogen and their relationships to earthquake distribution, contemporary strain field, and Cenozoic volcanism: Geosphere, v. 5, p. 199–214, doi: 10.1130/GES00217.1.

Taylor, M., Yin, A., Ryerson, F., Kapp, P., and Ding, L., 2003, Conjugate strike-slip faulting along the Bangong-Nujiang suture zone accommodates coeval east-west extension and north-south shortening in the interior of the Tibetan Plateau: Tectonics, v. 22, 1044, doi: 10.1029/2002TC001361.

Thatcher, W., 2007, Micoplate model for the present-day deformation of Tibet: Journal of Geophysical Research, v. 112, B101401, doi: 10.1029/2005JB004244.

Thiede, R.C., Arrowsmith, J.R., Bookhagen, B., McWilliams, M., Sobel, E.R., and Strecker, M.R., 2006, Dome formation and extension in the Tethyan Himalaya, Leo Pargil, northwest India: Geological Society of

America Bulletin, v. 118, p. 635–650, doi: 10.1130/B25872.1.

Valli, F., Arnaud, N., Leloup, P.H., Sobel, E.R., Mahéo, G., Lacassin, R., Guillot, S., Li, H., Tapponnier, P., and Xu, Z., 2007, Twenty million years of continuous deformation along the Karakorum fault, western Tibet: A thermochronological analysis: Tectonics, v. 26, TC4004, doi: 10.1029/2005TC001913.

Valli, F., Leloup, P., Paquette, J., Arnaud, N., Li, H., Tapponnier, P., Lacassin, R., Guillot, S., Liu, D., and Deloule, E., 2008, New U-Th/Pb constraints on timing of shearing and long-term slip-rate on the Karakorum fault: Tectonics, v. 27, TC5007, doi: 10.1029/2007TC002184.

Vannay, J., and Steck, A., 1995, Tectonic evolution of the High Himalaya in Upper Lahul (NW Himalaya, India): Tectonics, v. 14, p. 253–263, doi: 10.1029/94TC02455.

Vergnolle, M., Calais, E., and Dong, L., 2007, Dynamics of continental deformation in Asia: Journal of Geophysical Research, v. 112, B11403, doi: 10.1029/2006JB004807.

Wang, Q., Zhang, P.Z., Niu, Z.J., Freymueller, J.T., Lai, X., Li, Y.X., Zhu, W.Y., Liu, J.N., Bilham, R., and Larson, K.M., 2001, Present-day crustal deformation in China constrained by global positioning system measurements: Science, v. 294, p. 574–577, doi: 10.1126/science.1063647.

Williams, H., Turner, S., Kelley, S., and Harris, N., 2001, Age and composition of dikes in Southern Tibet: New constraints on the timing of east-west extension and its relationship to postcollisional volcanism: Geology, v. 29, p. 339–342, doi: 10.1130/0091-7613(2001)029<0339:AACODI>2.0.CO;2.

Wu, C., Nelson, K., Wortman, G., Samson, S., Yue, Y., Li, J., Kidd, W., and Edwards, M., 1998, Yadong cross structure and South Tibetan Detachment in the east central Himalaya (89°–90°E): Tectonics, v. 17, p. 28–45, doi: 10.1029/97TC03386.

Yin, A., 2000, Mode of Cenozoic east-west extension in Tibet suggesting a common origin of rifts in Asia during the Indo-Asian collision: Journal of Geophysical Research, v. 105, no. B9, p. 21,745–21,759, doi: 10.1029/2000JB900168.

Yin, A., and Harrison, T.M., 2000, Geologic evolution of the Himalayan-Tibetan orogen: Annual Review of Earth and Planetary Sciences, v. 28, p. 211–280, doi: 10.1146/annurev.earth.28.1.211.

Yin, A., Kapp, P., Murphy, M., Manning, C.E., Harrison, T.M., Din, L., Xiguang, D., and Chunming, W., 1999a, Significant late Neogene east-west extension in north Tibet: Geology, v. 27, p. 787–790, doi: 10.1130/0091-7613(1999)027<0787:SLNEWE>2.3.CO;2.

Yin, A., Harrison, T.M., Murphy, M.A., Grove, M., Nie, S., Ryerson, F.J., Feng, W.X., and Le, C.Z., 1999b, Tertiary deformation history of southeastern and southwestern Tibet during the Indo-Asian collision: Geological Society of America Bulletin, v. 111, p. 1644–1664, doi: 10.1130/0016-7606(1999)111<1644:TDHOSA>2.3.CO;2.

Zhang, P., Shen, Z., Wang, M., Gan, W., Bürgmann, R., Molnar, P., Wang, Q., Niu, Z., Sun, J., and Wu, J., 2004, Continuous deformation of the Tibetan Plateau from global positioning system data: Geology, v. 32, p. 809–812, doi: 10.1130/G20554.1.

Zhang, R., Murphy, M.A., Lapen, T.J., Sanchez, V., and Heizler, M., 2010, Late Eocene crustal thickening followed by Early-Late Oligocene extension along the India-Asia suture zone: Evidence for cyclicity in the Himalayan orogen, *in* Leech, M.L., et al., eds., Proceedings of the 25th Himalaya-Karakoram-Tibet Workshop: U.S. Geological Survey Open-File Report 2010–1099, 2 p., http://pubs.usgs.gov/of/2010/1099/zhangmurphy/.

Manuscript Received 28 April 2010
Revised Manuscript Received 1 November 2010
Manuscript Accepted 24 November 2010